JOURNAL OF GEOPHYSICAL RESEARCH, VOL. 104, NO. C10, PAGES 23,337–23,355, OCTOBER 15, 1999

Importance of ice-ocean interactions for the global ocean circulation: A model study

H. Goosse and T. Fichefet

Institut d'Astronomie et de Géophysique G. Lemaître, Université Catholique de Louvain, Louvain-la-Neuve, Belgium

Abstract. Numerical experiments are conducted with a coarse-resolution global ice-ocean model in order to determine to what degree the sea ice–ocean exchanges of heat, salt/freshwater, and momentum control the general circulation of the world ocean on long timescales. These experiments reveal that the formation of North Atlantic Deep Water (NADW) in the model results from the strong heat losses that occur at the oceanic surface in the high-latitude North Atlantic. The large-scale ice-ocean interactions have nearly no influence on this process. In particular, neglecting the freshwater flux associated with the southward ice transport at Fram Strait does not impact seriously on the salinity of the Greenland and Norwegian Seas. At equilibrium the absence of this freshwater flux is balanced by an enhanced oceanic freshwater transport from the Arctic. Furthermore, it appears that the model NADW formation does not critically depend on the media (ice or ocean) transporting the freshwater. Besides, both the salt/freshwater and heat exchanges between sea ice and ocean are crucial in the Southern Ocean for the deep water production, properties, and export. The large amount of brine released during ice formation on the model Antarctic continental shelf leads to very high salinities there. The resulting dense shelf waters are then transported toward great depths after some mixing with ambient waters, finally forming the Antarctic Bottom Water body. On the other hand, the net ice melting associated with ice convergence in some areas, such as the southwestern Pacific, stabilizes the water column and forbids deep mixing in these regions. Furthermore, the contact with the ice imposes that the polar surface waters must be maintained very close to their freezing point temperature. Our results suggest that this process takes an important part in increasing the density of the Antarctic Bottom Water. We also show that the modifications of the stress at the ocean surface induced by the internal ice stress have only a regional effect.

1. Introduction

Ice-ocean interactions impact on both sea ice and ocean evolutions since they determine the fluxes of freshwater/salt, heat, and momentum at the surface of the polar oceans as well as the conditions at the bottom of the ice pack. Process studies performed with simplified models (generally one- or two-dimensional) have allowed some insight into the physical mechanisms responsible for these ice-ocean exchanges [e.g., *Martinson*, 1990; *Holland et al.*, 1997]. Models have also enlightened their importance at the regional scale for the ocean circulation and ice extent [e.g., *Hibler and Bryan*, 1987; *Häkkinen*, 1993; *Holland et al.*, 1996].

The influence of the ice-ocean interactions on the global ocean circulation deserves some attention as well because a significant part of the world ocean's water masses acquire their characteristics at latitudes where sea ice processes can play a role. For instance, in the Southern Ocean the high salinities on the Antarctic continental shelf are a consequence of the strong ice production and subsequent brine rejection prevailing there. This salty and dense shelf water tends to sink along the continental slope after mixing with surrounding waters [*Foster and Carmack*, 1976; *Gordon*, 1991], forming the Antarctic Bottom Water (AABW) that occupies the bottom of the world ocean. The classical hypothesis for North Atlantic Deep Water (NADW) formation is deep convection in the Labrador Sea and in the Greenland-Iceland-Norwegian (GIN) Seas [e.g., *Killworth*, 1983; *Morawitz et al.*, 1996] caused by intense cooling of relatively warm and saline surface waters of tropical origin. Recently, *Mauritzen* [1996] has proposed an alternative scheme in which a more gradual heat loss to the atmosphere in the Norwegian Sea enhances the water density there. This dense water then circulates at intermediate depths in the GIN Seas and in the Arctic, modifying its properties by mixing with ambient waters before being exported southward across the Iceland-Scotland Ridge. Even though sea ice does not play a direct role in both of these schemes, ice formation in these areas has been suggested to be an efficient mechanism for the preconditioning of the water column, which makes deep mixing more likely to occur [*Visbeck et al.*, 1995]. On the other hand, strong ice transport toward the zones of deep water formation in the northern North Atlantic could stabilize the water column and reduce convection [*Aagaard and Carmack*, 1989; *Häkkinen*, 1993].

Because of the low thermal conductivity of sea ice, the oceanic heat loss to the atmosphere during winter in ice-covered seas is much lower than in regions where the ocean is ice-free. The presence of sea ice has thus a stabilizing effect. Indeed, in ice-free areas located at high latitudes, such as the open ocean polynyas, the strong surface heat losses can destabilize the ocean over a great depth, thus contributing to the deep water renewal [e.g., *Martinson*, 1990; *Gordon*,

Paper number 1999JC900215.
0148-0227/99/1999JC900215$09.00

1991]. Nevertheless, the thermal effect of sea ice is not only a stabilizing one. Indeed, the maximum density of seawater, at a given salinity and pressure, is reached at the freezing point temperature. As a consequence, lowering the temperature until the freezing point by contact with the ice can take part in the density increase necessary to reach the bottom layers.

In ice-covered seas the stress at the ocean surface is modified compared to the air stress because of the ice momentum balance that includes, in addition to those two stresses, the internal ice stress, the Coriolis force, and the effect of the surface tilt [e.g., *Hibler*, 1979]. The last two components have generally a weak magnitude [e.g., *Steele et al.*, 1997], so in case of a loose ice pack the ice-ocean stress is close to the air-ice stress. By contrast, in regions where the ice interaction is strong, as in the central Arctic, the ice-ocean stress is much lower than the air-ice stress. This reduction of the stress at the ocean surface can affect the oceanic circulation, with a potential influence on the oceanic heat and freshwater transports at high latitudes and/or on the water properties in the regions of deep water formation.

In the present study these large-scale effects of the exchanges of freshwater/salt, heat, and momentum between ice and ocean are evaluated by performing numerical experiments with a coarse-grid, global, three-dimensional ice-ocean model. Our goal is to understand the physical behavior of the model and to compare the processes identified to what is known or hypothesized about the real world from observations or other sources. The short-term objective is not to improve the model performance, even though a better understanding of the model would certainly help to reduce its inaccuracies. As a consequence, we do not vary the model parameters inside their range of uncertainties or test the influence of different representations of a particular process on the quality of the model results as classically done [e.g., *Kim and Stössel*, 1998]. Indeed, in such experiments the response of the model does not generally provide a clear picture considering a particular process. Rather, we perform idealized experiments designed to isolate as much as possible the influence of the fluxes at the ice-ocean interface on the world ocean's circulation (Table 1). In the first one, devoted to the analysis of the role of the mass transfers between ice and ocean, the ice-ocean exchange of freshwater/salt associated with ice melting/freezing is neglected (no salt flux experiment, NSF). Totally suppressing the heat flux at the ice base would allow ice formation over relatively warm water if the atmospheric cooling is sufficient. As this is not very realistic, it has been decided only to reduce the heat exchange coefficient between ice and ocean (low heat transfer experiment, LHT). Another effect of the ice coverage is to maintain the oceanic surface at the freezing point over a relatively large area. An experiment has been carried out in which this temperature is increased (freezing point temperature experiment, FPT). Finally, an experiment is conducted in which the wind stress is imposed directly at the ocean surface (stress at the ocean surface equal to wind stress experiment, STW).

Contrary to the heat and momentum fluxes at the ice-ocean interface, the influence of salt/freshwater exchange between ice and ocean has been studied before with global ocean models [e.g., *Toggweiler and Samuels*, 1995a; *England and Hirst*, 1997] or global coupled ice-ocean models [e.g., *Legutke et al.*, 1997; *Goosse et al.*, 1997b; *Stössel et al.*, 1998]. Taking into account the impact of sea ice on the freshwater/salt flux in ocean-only models is problematic, and the way it was done in the past could profoundly affect the results. Nevertheless, all these studies reveal a significant influence of the exchanges of mass between ice and ocean on deep water production and export in the Southern Ocean. A similar run has been included here (NSF) for completeness and because it is the first time that such an experiment has been performed using a coupled ice-ocean model with no restoring in polar regions at any time of the year and which yields a reasonable simulation of the Arctic and Antarctic ice packs. Furthermore, the results of the previous studies [*Goosse et al.*, 1997b; *Stössel et al.*, 1998] were different in some respects, and possible reasons for these discrepancies are discussed. Finally, the analysis of experiment NSF is performed in both hemispheres, contrary to the previous studies that mainly focused on the Southern Ocean.

A limitation of the present study is the use of a horizontal resolution of only 3°. Because of this coarse resolution, it is possible that the model reference run is outside the realm of response that is characteristic of the real ice-ocean system. Thus the results obtained from removing individual components of the system must be interpreted with caution. Ideally, such process studies should be conducted with eddy-resolving global ice-ocean models. Present-day computer capacities, however, do not yet allow such models to be integrated toward near-equilibrium, not even for a single experiment [*Kim and Stössel*, 1998]. So, they are not yet suited for investigating the impact of sea ice-related processes on the deep ocean. At this stage of computer advancement, our experiments could be considered as complementary to the ones performed with high-resolution global or local models. The latter types of experiments give precise information on the physics of ice and ocean on short timescales but do not allow investigation of the slow adjustments. On the other hand, coarse-grid models can provide clues about those long timescales even though they are not able to represent the details of the circulation. Furthermore, it should be noted that global climate-modeling studies are still performed with non eddy-resolving ice-ocean components [see *Houghton et al.*, 1996]. We therefore believe it is of prime importance to analyze the physical behavior of these models thoroughly.

Table 1. List of Experiments

Abbreviation	Experiment
CTR	control experiment
NSF	no salt/freshwater flux between ice and ocean
LHT	lower heat transfer coefficient between ice and ocean (reduction by a factor 5)
FPT	freezing point temperature increased by 1°C
STW	wind stress applied directly at ocean surface

The paper is organized as follows. The model, forcing, and experimental design are described in sections 2 and 3. The control experiment (CTR) is briefly discussed in section 4. Sections 5-7 are devoted to the analysis of the sensitivity experiments. Concluding remarks are finally given in section 8.

2. Description of the Ice-Ocean Model

The Coupled Large-scale Ice-Ocean (CLIO) model [*Goosse et al.*, 1997a,b, 1999] results from the coupling of a global, free surface ocean general circulation model (OGCM) [*Deleersnijder and Campin*, 1995; *Campin and Goosse*, 1999] with a comprehensive sea ice model [*Fichefet and Morales Maqueda*, 1997]. Only a brief description of the model characteristics is provided here. Further information can be found in the above mentioned references. The sea ice model has representations of both thermodynamic and dynamic processes [*Fichefet and Morales Maqueda*, 1997]. It takes into account the sensible and latent heat storage in the snow-ice system and the presence of leads and polynyas within the ice pack. Ice dynamics is computed by assuming that sea ice behaves as a viscous plastic continuum [*Hibler*, 1979]. The OGCM is a primitive equation model resting on usual approximations. The parameterization of vertical mixing [*Goosse et al.*, 1999] is based on a simplified version of the *Mellor and Yamada*'s [1982] level-2.5 model. Whenever the vertical density profile is unstable, the vertical diffusivity is enhanced to 10 $m^2 s^{-1}$. The horizontal eddy diffusivity and viscosity are set equal to 150 and 10^5 $m^2 s^{-1}$, respectively. The horizontal resolution is of 3° x 3°, and there are 20 unequally spaced vertical levels in the ocean.

In addition, the parameterization of dense water flow down topographic features of *Campin and Goosse* [1999] is included in this version of the model. It works as follows: if the density at the bottom of a shallow region near a bathymetric step is higher than the one at the same depth in the neighboring deeper region, a water transport from the shallow area to the deeper one occurs at a rate proportional to the horizontal density gradient. This water flows down the slope (represented as a vertical wall in the model) until a depth at which its density is equal to the one of ambient waters or directly to the bottom if this condition is never met.

Since this study focuses on the role of ice-ocean interactions, more details about the way they are parameterized in the model are given below. The ice-ocean stress τ_{iw} is taken to be a quadratic function of the difference between the ice velocity $\boldsymbol{u}_i$ and the ocean surface velocity $\boldsymbol{u}_w$:

$$\tau_{iw} = \rho_0 c_{iw} |\boldsymbol{u}_i - \boldsymbol{u}_w| (\boldsymbol{u}_i - \boldsymbol{u}_w) , \qquad (1)$$

where ρ_0 is a reference seawater density and c_{iw} is a drag coefficient ($c_{iw} = 5 \times 10^{-3}$).

Following *McPhee* [1992], the sensible heat flux from the ocean to the ice, F_{wi}, is taken to be proportional to the difference of temperature between the surface layer, T_w, and its freezing point, T_{Freez}, and to the friction velocity u_{*io}:

$$F_{wi} = \rho_o c_{pw} c_h u_{*io} (T_w - T_{\mathrm{Freez}}) , \qquad (2)$$

where c_{pw} is the specific heat of seawater and c_h is a coefficient set equal to 0.006 [*McPhee*, 1992]. T_{Freez} is a function of the sea surface salinity as given by *Fichefet and Morales Maqueda* [1997].

In the model the mass exchanges between ice and ocean are represented in terms of an equivalent salt flux:

$$F_{salt} = S_w \left(\frac{\partial m_s}{\partial t} \right) + (S_w - S_i) \left(\frac{\partial m_i}{\partial t} \right) , \qquad (3)$$

where S_i is the sea ice salinity, assumed to be constant (4 practical salinity units (psu)), S_W is a reference seawater salinity (34.7 psu), and m_S and m_i are the masses of snow and ice per unit area, respectively. The first term on the right-hand side of (3) simulates the freshwater flux to the ocean due to snow melting by a negative salt flux. The second one mimics the brine rejection and nearly fresh water flux associated with ice formation and melting, respectively.

3. Forcing and Experimental Design

The model is dynamically driven by the climatological monthly wind stresses τ_S of *Trenberth et al.* [1989] between 15°S and 15°N and of *Hellerman and Rosenstein* [1983] out of this latitude band. Using a monthly wind forcing tends to underestimate the wind energy transfer to the ocean, with potential consequences on the intensity of mixing in the upper layers. In order to limit this problem the friction velocities are directly taken from the climatology computed with daily data [*Trenberth et al.*, 1989] instead of calculating it from the monthly mean wind stress fields. Below the ice it is assumed that the square of the friction velocity is reduced by a factor $|\tau_s|/|\tau_{iw}|$ to take into account the effect of ice dynamics. The surface fluxes of heat are determined from atmospheric data by using the classical bulk formulas described by *Goosse* [1997]. Input fields consist of monthly climatological surface air temperatures [*Taljaard et al.*, 1969; *Crutcher and Meserve*, 1970], cloud fractions [*Berliand and Strokina*, 1980], air relative humidities [*Trenberth et al.*, 1989], and surface winds (same sources as for wind stresses). Evaporation/sublimation is derived from the turbulent flux of latent heat. Precipitation and freshwater inflow from the largest rivers are prescribed according to the monthly climatologies of *Xie and Arkin* [1996] and *Grabs et al.* [1996], respectively. For smaller rivers the annual runoff values of *Baumgartner and Reichel* [1975] are utilized. In addition, a relaxation toward observed annual mean salinities [*Levitus*, 1982] is applied in the 10 m thick surface grid box with a time constant of 60 days. This correction is introduced in order to prevent any salinity drift caused by inaccuracies in the precipitation and runoff data and in the evaporation computed by the model. To give an order of magnitude, this restoring induces a freshwater flux equivalent to 0.18 m of water per year if the difference between the simulated salinity and Levitus' data is equal to 0.1 psu.

A particularity of the present study compared to previous experiments carried out with the CLIO model [e.g., *Goosse et al.*, 1997a,b, 1999] is the absence of salinity relaxation in polar regions. This modification in the model forcing has been introduced because a link to climatological salinity in high latitudes can make the interpretation of the results issued from the sensitivity experiments more difficult. The problem would probably be the most significant for the study of the role of the mass exchanges between ice and ocean (section 5) since the flux associated with the relaxation could reach at some locations a magnitude similar to the physical flux obtained by (3). If the relaxation were applied everywhere, the changes of the relaxation flux in polar regions between the

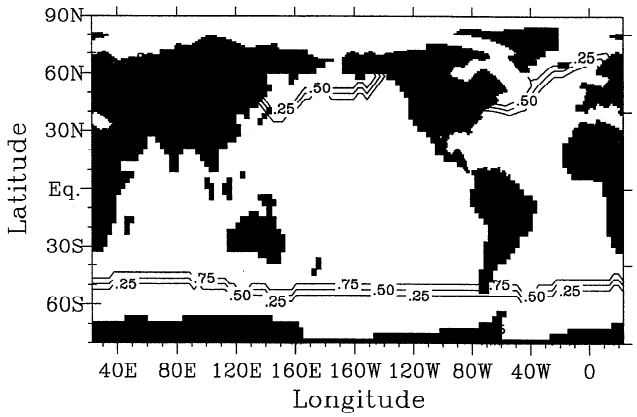

Figure 1. Distribution of the relative intensity of the relaxation on surface salinity (between 0 and 1). Contour interval is 0.25.

control and sensitivity experiments might mask the effect we want to highlight. Because of similar arguments, *Stössel et al.* [1998] apply relaxation toward observed salinities only in ice-free grid cells, the relaxation being equal to zero when ice is present. This means that in seasonally ice-covered regions, relaxation is applied in summer but not in winter.

A different approach is chosen here: no relaxation is applied at any time of the year in the regions where ice can appear. This zone is diagnosed from the maximum ice extent obtained in a control experiment with surface relaxation everywhere, increased by one grid point (~300 km) in each direction for safety. Outside of this region, the relaxation strength increases linearly over a four grid point buffer zone (Figure 1) to avoid very strong and localized relaxation fluxes where water is advected from a zone without relaxation (which can thus have surface properties quite different than the observed ones) to a zone where relaxation is applied. With these requirements, no relaxation is applied southward of 55°S, the distribution being less zonal in the Northern Hemisphere (see Figure 1).

To reduce the errors in surface salinity, some "flux corrections" are applied to the freshwater forcing in the Southern Ocean, where uncertainties in precipitation are quite large [e.g., *Xie and Arkin*, 1996]. Between 60° and 51°S in the South Atlantic (90°W - 30°E) and south Indian Oceans (30°E - 150°E) the precipitation rates have been increased by 0.25 and 0.35 m yr^{-1}, respectively. Those values are of the order of magnitude of the differences between the existing climatologies. For instance, in the south Indian Ocean, *Jaeger*'s [1976] precipitation climatology gives an averaged value that is 0.21 m yr^{-1} higher than *Xie and Arkin*'s [1996] one, and *Legates and Willmott* [1990] provide a value that is 0.47 m yr^{-1} greater than that of *Xie and Arkin* [1996]. In the South Atlantic the differences are of 0.16 and 0.34 m yr^{-1}, respectively. Another correction is applied in the Arctic basin (including peripheral seas) where the river runoff amounts to an annual mean of 0.08 Sv using the data mentioned above. As the estimates are generally a little higher (e.g., 0.12 Sv for *Cattle* [1985] and 0.10 Sv for *Aagaard and Carmack* [1989]), the total freshwater flux to the Arctic has been enhanced by 0.03 Sv, this amount being uniformly distributed over the basin. All those corrections are constant throughout the year.

The experiments are analyzed after a 1000 year integration under this forcing, starting from an equilibrium state in robust diagnostic mode (i.e., with relaxation on salinity and temperature to *Levitus*'[1982] observations at all depths). The results discussed below are averages made over the last 10 years of integration except for NSF for which an average over the last 100 years has been performed (see section 5).

4. Control Experiment

Some results of the control experiment (hereafter referred to as CTR) that can be directly helpful for the discussion of the sensitivity experiments are briefly presented now. Complementary information about the general model performance is given by *Goosse et al.* [1997a,b, 1999].

Figure 2 indicates that the ice extent in both hemispheres is reasonably well simulated. In the Northern Hemisphere, only some minor differences between the model and observations are noticed. For instance, in March some ice is present off the north coast of Norway, which is contrary to the observations, while the predicted ice extent is underestimated south of Spitzbergen. The cause of these discrepancies is the wrong path of the ocean surface currents in these regions: rather than flowing along the Norwegian coast toward the Barents Sea, as observed, the simulated Norwegian Current flows directly northward and enters the Arctic Ocean east of Spitzbergen. This current carries warm Atlantic waters, inducing strong ice melting south of Spitzbergen in the model. On the contrary, the heat transport to the Barents Sea is too weak, allowing ice to be maintained there. Considering the summer ice extent, the only significant difference between the model and observations is the underestimation in the Kara and Laptev Seas.

The modeled winter ice thickness increases from ~3 m off eastern Siberia to a maximum of ~6 m north of Greenland and the Canadian Archipelago (Figure 3a). This pattern qualitatively agrees with that derived from submarine sonar measurements [*Bourke and McLaren*, 1992], even if the ice thickness on the Siberian side appears to be a little overestimated. Another interesting diagnostic is the ice volume transport through Fram Strait. In CTR it amounts to 6.7 x 10^{-2} Sv of ice on an annual average (i.e., 2113 km^3 y^{-1}), which is at the lower bound of current estimates [*Aagaard and Carmack*, 1989; *Thomas et al.*, 1996] and very close to the results found by *Häkkinen* [1993] using a model of the Arctic circulation with a much finer resolution than ours. By contrast, the annual mean southward transport of freshwater by the ocean at Fram Strait (0.07 Sv) is overestimated compared to the estimate of *Aagaard and Carmack* [1989] or *Steele et al.* [1996].

In the central Arctic the flux of sensible heat flux from the ocean to the ice, excluding the contribution from leads, ranges between 0 and 3 Wm^{-2} throughout the year (Figure 4a), in good agreement with the available observations [e.g., *McPhee and Untersteiner,* 1982]. This flux reaches much higher values in peripheral seas, such as the Labrador Sea, the Bering Sea, or the Greenland Sea, with a maximum of 100 Wm^{-2} during winter months north of Iceland. This high value is due to the inflow of warm Atlantic waters below the ice in this sector. In the Fram Strait area and in the southern Barents Sea the oceanic heat flux is rather low and probably underestimated since the model is neither able to represent the West Spitzberg Current nor the flow of Atlantic waters along the north coast of Norway, as already mentioned.

In the Southern Hemisphere the simulated winter ice extent is overestimated in the Pacific sector and between 45° and

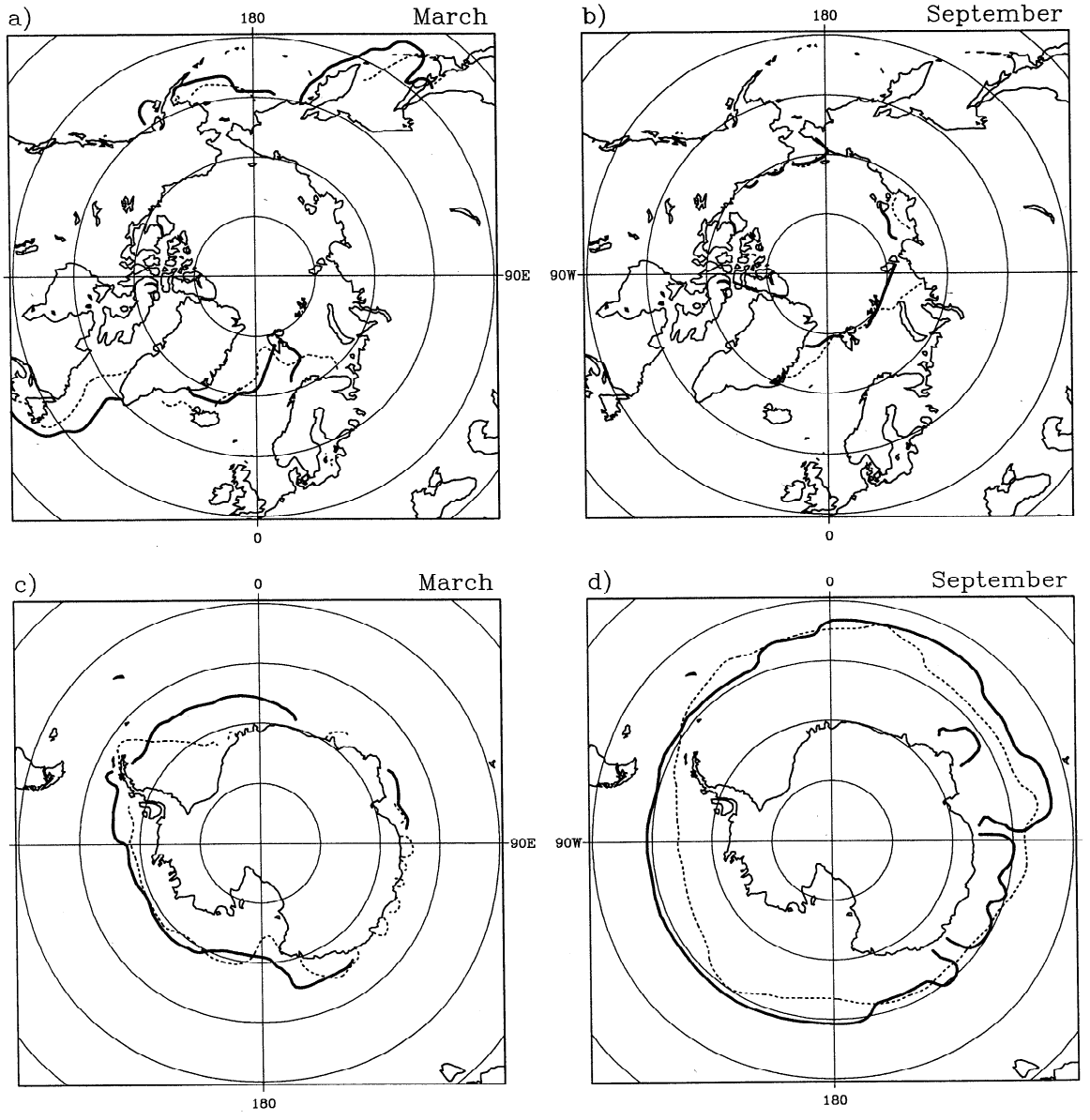

Figure 2. Location of the ice edge defined as the 15% ice concentration contour: (a) Northern Hemisphere in March, (b) Northern Hemisphere in September, (c) Southern Hemisphere in March, and (d) Southern Hemisphere in September. The solid line represents the model results for the control experiment (CTR), while the dashed line represents the observations of *Gloersen et al.* [1992].

90°E. On the other hand, it is underestimated between 90° and 150°E. This underestimation is associated with open ocean convection reaching a depth of more than 2000 m in this area; the convection brings heat from the deep ocean to the surface, which generates ice melting (Figure 4b). This too strong open ocean convection in the Southern Ocean seems to be a problem of most ice-ocean models [*Legutke et al.*, 1997; *Stössel et al.*, 1998], but it must be stressed that this phenomenon is quite restricted here and has only a weak impact on the sea ice distribution. One can also notice the presence of a wide polynya near 45°E, a region where such features have been frequently observed [e.g., *Comiso and Gordon*, 1987]. The mechanism responsible for the open ocean convection occuring there in the model and its link with polynya formation are analyzed thoroughly in a forthcoming paper (H. Goosse and T. Fichefet, Open-ocean convection and polynya formation in a large-scale ice-ocean model, submitted to *Tellus*, 1999).

In summer the only problem is that the ice extends too far northward in the eastern Weddell Sea. This error may be attributed to atmospheric forcing since various authors using different models [e.g., *Stössel et al.*, 1990; *Fichefet and Morales Maqueda*, 1997] have obtained the same kind of behavior when utilizing *Taljaard et al.*'s [1969] air temperatures as the forcing.

The modeled mean ice thickness in winter in the Southern Ocean is a little bit lower than 1 m (Figure 3b), in general accordance with observations [e.g., *Budd*, 1991]. Nevertheless, the ice thickness is overestimated on the western side of the Antarctic Peninsula because of too strong a wind-driven ice convergence in the model.

High values of the oceanic heat flux are noticed in regions

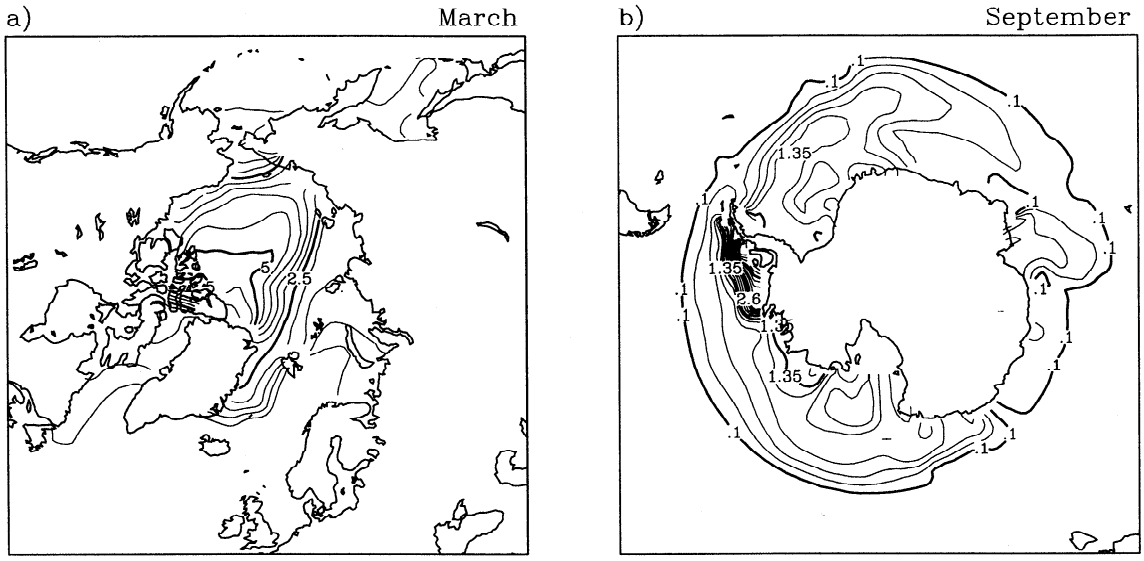

Figure 3. Winter ice thickness in CTR: (a) Northern Hemisphere in March, where the contour interval is 0.5 m, and (b) Southern Hemisphere in September, where the contour interval is 0.25 m.

of the Southern Hemisphere that receive a direct inflow of relatively warm water from the Antarctic Circumpolar Current (ACC), such as north of the Weddell Gyre or the Indian sector of the Southern Ocean (Figure 4b). In the latter area the flux is overestimated between 90° and 150°E because of the too intense mixing occurring there in the model, resulting in too thin an ice cover (see above). In the southeastern part of the Weddell Sea, thanks to the inflow of water coming from the ACC by the southern limb of the Weddell Gyre, the oceanic heat flux is also quite strong, with annual mean values greater than 15 Wm^{-2}. Note that these values are close to the estimates of *Gordon and Huber* [1990]. The western Weddell Sea is more remote from the sources of warm water. As a consequence, the annual mean heat flux is lower than 10 Wm^{-2} in this area in accordance with the observational data of *Lytle and Ackley* [1996]. The eastern Ross Sea also displays strong heat fluxes at the ice base, with maximum values of 50 Wm^{-2}. This is caused by an intense upwelling of warm Circumpolar Deep Water (CDW) and contributes to the opening of a spring Ross Sea polynya in the model [*Fichefet and Goosse*, 1999].

In the Northern Hemisphere the model simulates deep convection in the GIN Seas and in the Labrador Sea close to the southern tip of Greenland (Figure 5), in qualitative agreement with the observations [*Killworth*, 1983]. The mixing is also intense in the eastern Bering Sea, but the convection is limited to a depth of 1000 m there and only takes part in the renewal of the model Pacific intermediate waters. In the Southern Ocean, on the continental shelf of the Ross Sea and Adélie Coast–Wilkes Land (140°E to 160°W) and of the Weddell Sea (60°W to 30°E), convection reaches the model bottom, which is located in this area between 150 and 600 m. This is caused by the very strong ice production there,

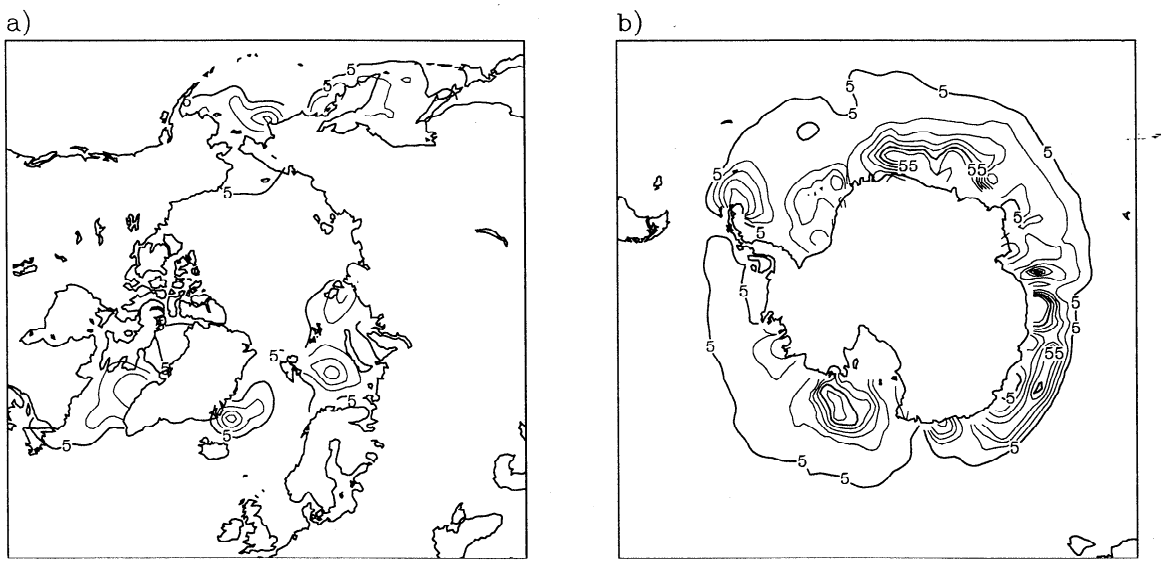

Figure 4. Annual mean oceanic heat flux at the ice base, excluding the contribution coming from leads, in (a) the Northern Hemisphere and (b) the Southern Hemisphere. The contour interval is 10 W m^{-2}.

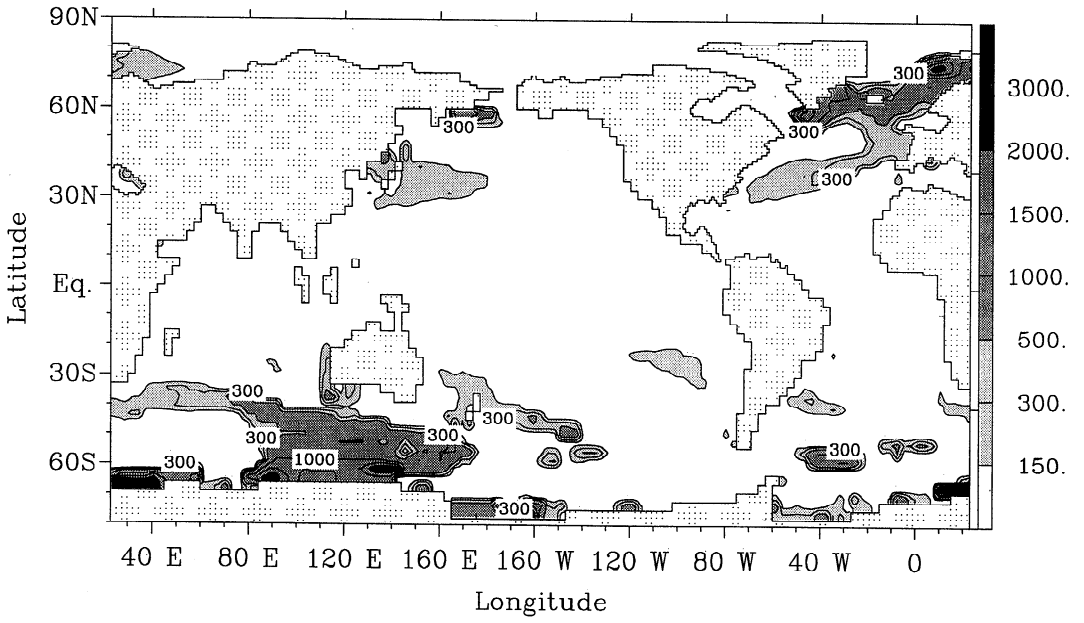

Figure 5. Maximum depth of vertical convection in CTR. The contour levels are drawn at 150, 300, 500, 1000, 1500, 2000, and 3000 m.

leading to a salt flux associated with ice formation equivalent to -1 to -3 m of freshwater per year [*Goosse et al.*, 1997b]. Therefore the surface salinity increases significantly, inducing a destabilization of the water column over its whole depth in winter. As already mentioned, deep convection is also simulated close to Antarctica between 20° and 40°E and between 80° and 120°E. In the Indian sector (and to a lesser extent in the Atlantic sector), the convection up to a depth of 750 m or more at 50°-60°S is not realistic. This problem is probably related to the too simple parameterization of the effect of subgrid-scale eddies [e.g., *England and Hirst*, 1997]. The convection there does not directly take part in AABW production but affects significantly the ventilation of the Southern Ocean [*Goosse et al.*, 1999].

In the model, AABW is formed by both open ocean convection and by the sinking of the dense water produced on the Antarctic continental shelf. The parameterization of downsloping flows, which induces an export of 6.2 Sv out of the shelf, is a major contributor to the latter mode of AABW renewal (for more details about the representation of this process in the model, see *Campin and Goosse* [1999]). In addition, the clockwise cell located close to Antarctica in Figure 6a, which has a maximum strength of 33 Sv, contributes to the tranport of the dense water toward the bottom of the Southern Ocean. Then this water is advected northward, the maximum intensity of the bottom cell at 30°S being of 17 Sv. Above the AABW the circulation is dominated by the NADW overturning, which has its two major sources in the GIN Seas and Labrador Sea. This overturning reaches a maximum strength of 25 Sv in the Atlantic, with 18 Sv of NADW being exported southward at 30°S (Figure 7a).

These results concerning NADW are within the range of current estimates, probably on the high side [*Schmitz*, 1995; *Macdonald and Wunsch*, 1996]. Besides, the AABW circulation seems to be too intense. For example, the NADW is observed to reach the bottom of the Atlantic north of 40°N, while in our experiment, AABW occupies the bottom of the whole Atlantic. This problem does not occur in previous runs performed with the model [*Goosse et al.* 1997a,b, 1999]. It is associated with the absence of relaxation in the high latitudes of the Southern Ocean, which tends to induce surface salinities in CTR ~0.15 psu higher than the observations of *Levitus* [1982] on a zonal average between 60° and 70°S. The salinity on the Antarctic continental shelf is also higher than in the previous runs with relaxation. These too high salinities in the Southern Ocean generate high densities there, causing the too strong production and export of AABW noticed in CTR.

5. Influence of the Freshwater and Salt Exchanges Between Ice and Ocean

The mass exchanges between ice and ocean have a profound influence on the vertical structure of the water column because the brine released during ice formation tends to increase the surface density and destabilize the system, while the influx of nearly fresh water into the ocean when sea ice melts has the opposite effect. The impact of this process on the world ocean's circulation is investigated in this section by performing a model experiment in which the fluxes of freshwater and salt associated with ice formation and melting are neglected (hereafter referred to as NSF). This amounts to assuming that sea ice has the same salinity as seawater. The other characteristics of the experiment remain the same as in CTR.

Contrary to all the other experiments, NSF displays a strong decadal variability, with a predominant timescale of the order of 25-50 years. This variability has its origin in the Southern Ocean, with periods of strong open ocean convection in winter followed by periods in which the winter ocean is much more stable. These changes of convection have consequences on the ice extent as well as on the deep water renewal. It is not the purpose of the present work to investigate the ocean and ice variabilities; so, a detailed

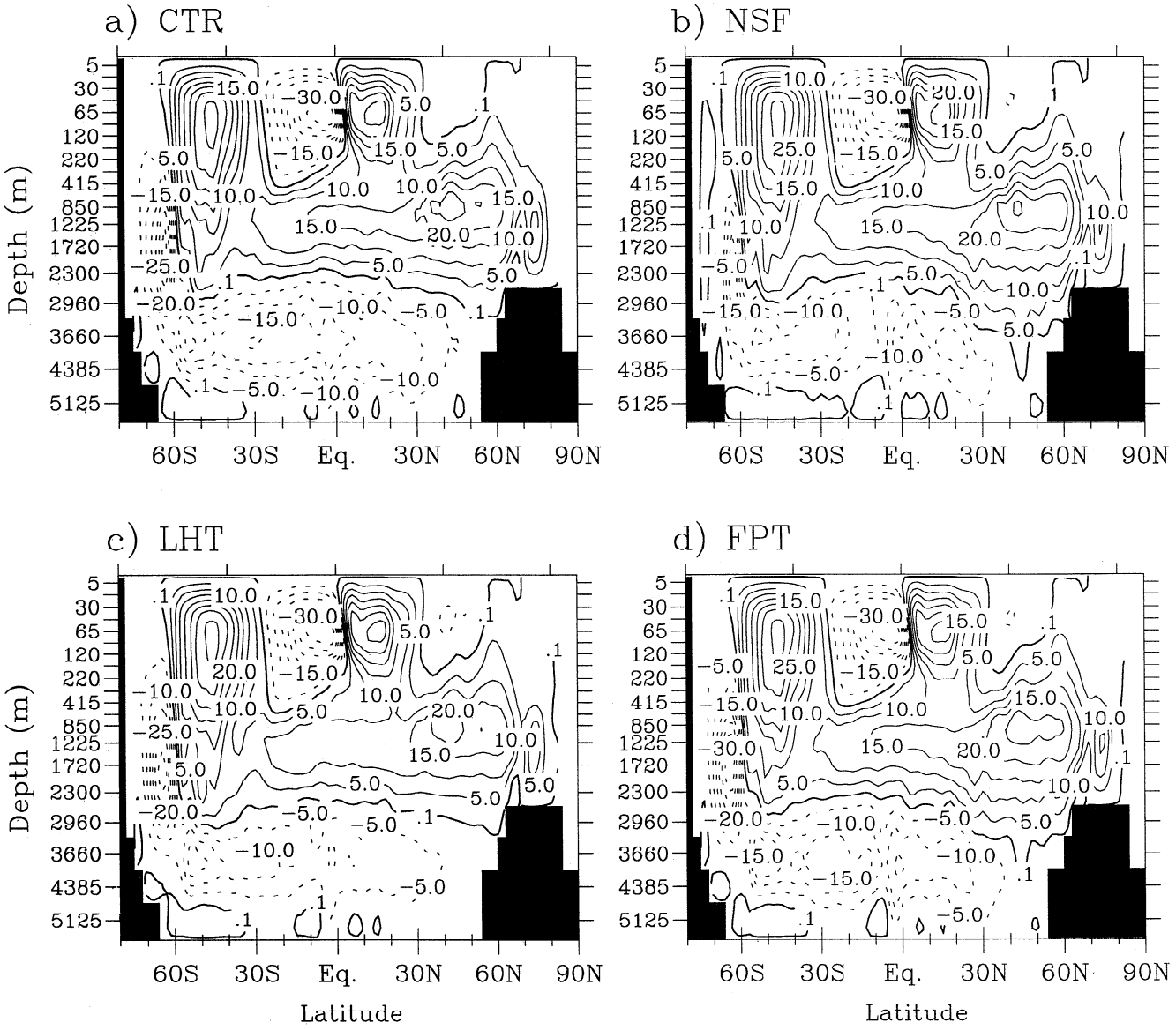

Figure 6. Zonally integrated meridional stream function in the global ocean: (a) CTR, (b) no salt flux experiment (NSF), (c) low heat transfer experiment (LHT), and (d) freezing point temperature experiment (FPT). The flow is clockwise around solid contours. The contour interval is 5 Sv.

analysis of this model feature is not performed. Results are averaged over the last 100 years of the integration in order to remove this variability. It must be noticed that averaging over the last 100 years instead of 10 years for the other experiments is of no consequence because of the near absence of interannual variability in these runs.

In NSF, there is generally a decrease in sea surface salinity compared to CTR in regions where net ice production takes place in CTR and an increase where net ice melting is observed in CTR. Over the Antarctic continental shelf the salinity decrease is strong, with differences greater than 1.5 psu in the Ross and Weddell Seas on an annual average (Figure 8). Even if the net ice production in the central Arctic is weaker than in the vicinity of Antarctica, the salinity decrease in NSF can reach 4 psu in the Arctic because it is a semienclosed basin where the influence of surface flux on the local salinity is high.

In some areas the changes in oceanic horizontal freshwater transport between the two experiments mask the differences in the local freshwater fluxes. For instance, off the west coast of Greenland, net ice melting occurs in CTR because of the ice export out of the Arctic through Fram Strait. However, a salinity decrease is observed in NSF compared to CTR. This is due to the advection of much fresher water from the Arctic in NSF, which overwhelms the effect of the decrease in the surface freshwater flux at this location.

The compensating influences of no freshwater transport by ice and of an increase in the oceanic freshwater transport are also important at large scale. Consider the freshwater budget of the ice-ocean system in a particular area, for instance, the central Arctic or the continental shelf of the Ross Sea: at equilibrium the net freshwater flux at surface due to river runoff, precipitation, and evaporation must be balanced by horizontal freshwater export out of the region. In CTR this

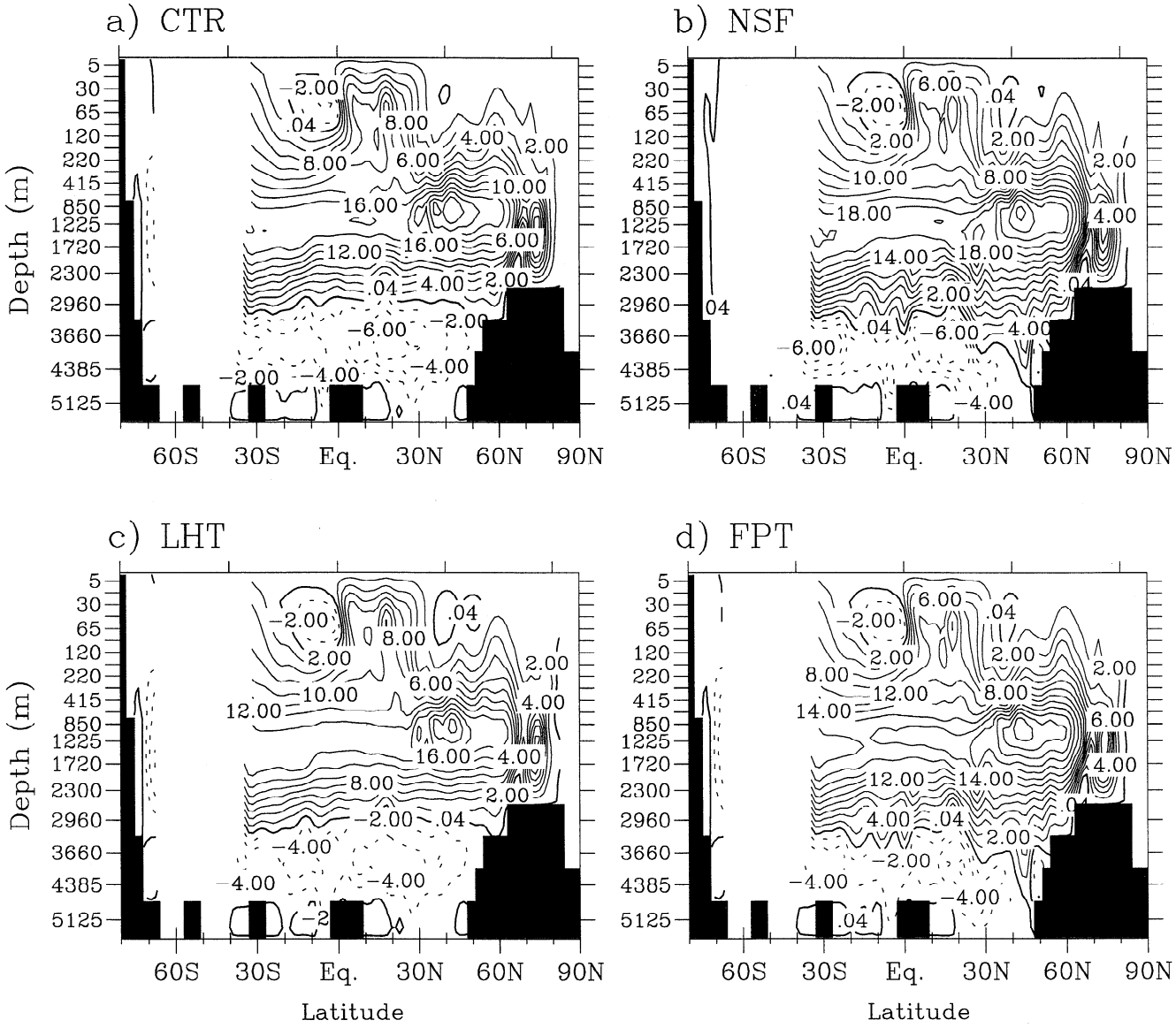

Figure 7. Zonally integrated meridional stream function in the Atlantic Ocean: (a) CTR, (b) NSF, (c) LHT, and (d) FPT. The flow is clockwise around solid contours. The contour interval is 2 Sv.

freshwater transport can be achieved by either the ocean or the ice, while in NSF, it can only be carried out by the ocean. As the total export remains the same in NSF and in CTR (runoff and precipitation being fixed and evaporation remaining nearly constant), the total oceanic export of freshwater must increase in NSF. This explains why the salinity of the GIN Seas as a whole does not increase in NSF. In CTR the ice and ocean transport 0.05 and 0.07 Sv of freshwater from the Arctic to the GIN Seas, respectively (see section 4). The freshwater transport associated with the southward ice motion at Fram Strait is eliminated in NSF, but this is balanced by an increase in the amount of freshwater carried out by the ocean (0.12 Sv in NSF), mainly because of the lower salinity in the Arctic. Nevertheless, the freshwater is not necessarily transported to the same locations by the ice or the ocean and some local changes can take place. In the GIN Seas the differences between the experiments are mainly located along the Greenland coast (Figure 8), with nearly no impact on the large-scale circulation. At other locations it can result in more dramatic changes, as discussed below.

The strong decrease in salinity over the Antarctic continental shelf induces a suppression of the convection there. Besides, at some open ocean locations, convection is still present and even intensifies (Figure 9), as in the southeastern Pacific. In this area, net ice melting of more than 1m yr^{-1} is observed in CTR because of ice transport convergence, generating a very stratified water column with a mixed layer always shallower than 100 m. In NSF the ice flow is not associated with a freshwater transport. As a result, the surface salinity increases in this sector, thus favoring deep convection. In the Northern Hemisphere the convection in NSF shows only small differences compared to CTR, as could have been deduced from the weak modifications of the surface salinity in the zones of convection (see Figures 8 and 9).

The overturning in NSF is profoundly modified close to Antarctica (Figure 6b), where the strong downwelling along

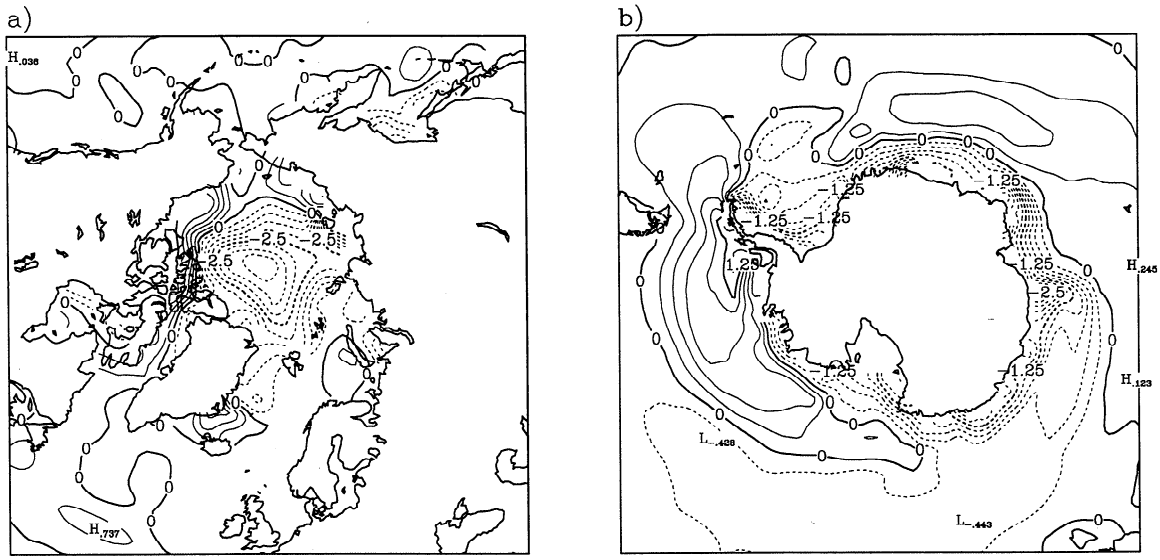

Figure 8. Difference of annual mean surface salinity between NSF and CTR (NSF-CTR): (a) Northern Hemisphere, where the contour interval is 0.5 psu, and (b) Southern Hemisphere, where the contour interval is 0.25 psu.

the continental slope observed in CTR has completely disappeared. The transport of dense water out of the continental shelf by the downsloping currents is also reduced to <0.5 Sv. However, downwelling is still present between 65° and 70°S, associated with the cooling due to open ocean convection in this latitude band. In addition, the intensity of the counterclockwise cell off the Antarctic continent is dramatically reduced, with the maximum decreasing from 33 Sv in CTR to <19 Sv in NSF. The outflow out of the Southern Ocean to the other basins close to the bottom also has a smaller magnitude: at 40°S the maximum of the bottom overturning cell is 12 Sv in NSF, whereas it amounts to 17 Sv in CTR. Furthermore, the northward propagation of AABW is weaker. In the Atlantic, north of 40°N, it no longer occupies the ocean bottom as in CTR, the bottom layers being mainly fed by NADW.

Besides, the NADW export at 30°S (see Figure 7b) increases slightly in NSF compared to CTR (+1.3 Sv). One could argue that this modification is due to changes in surface conditions in the North Atlantic. However, as mentioned above, the differences of surface salinity and convection between the two experiments are relatively weak there. Furthermore, in a former experiment (described by *Goosse et al.* [1997b]) in which the salt and freshwater fluxes associated with ice production and melting were neglected only in the Southern Hemisphere a similar increase in NADW export was simulated.

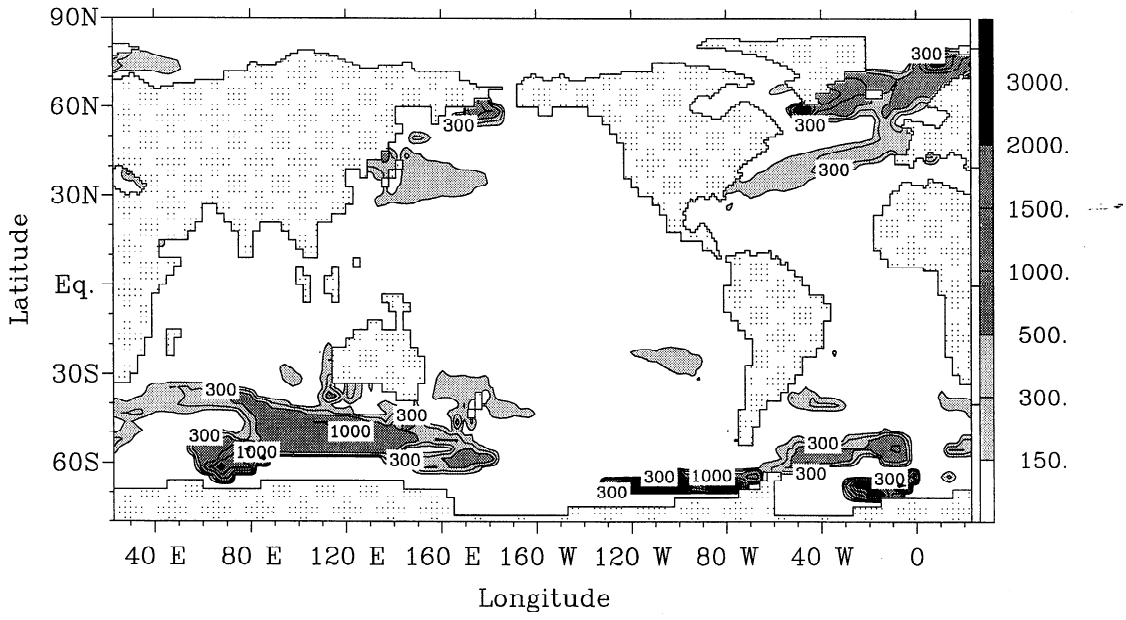

Figure 9. Depth of vertical convection in NSF. Contour levels are drawn at 150, 300, 500, 1000, 1500, 2000, and 3000 m.

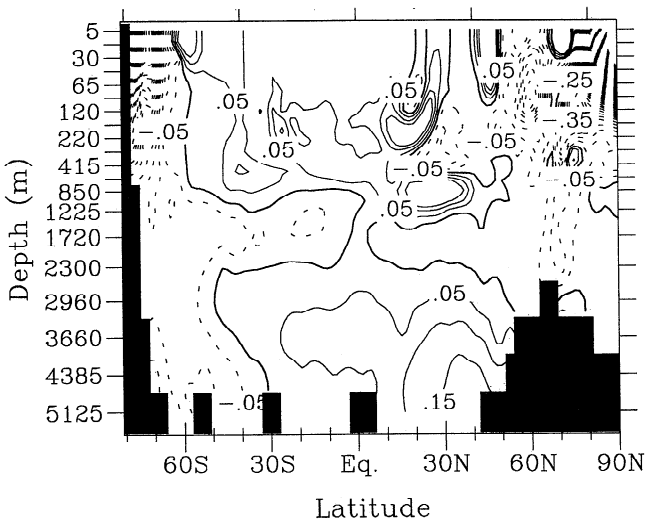

Figure 10. Difference of annual mean, zonally averaged salinity between NSF and CTR (NSF-CTR) in the Atlantic Ocean. The contour interval is 0.05 psu.

As a consequence, the NADW production seems to respond more to a change in the AABW circulation than to a local effect in the North Atlantic.

The absence of salt export from the Antarctic continental shelf generates a salinity decrease of the bottom water formed near Antarctica (Figure 10). On the other hand, in the Atlantic, there is a noticeable increase in salinity close to the bottom north of 30°S. This can seem strange since the salt rejected on the Antarctic continental shelf during ice formation is supposed to contribute to a salinity increase of the bottom water. *Toggweiller and Samuels* [1995a] and *Goosse et al.* [1997b] have estimated this effect to be ~0.05 psu on a global average. However, the inflow of salty NADW at great depths is stronger in NSF than in CTR. This induces a salt transport to the deep levels that compensates for the lack of salt transport from the Antarctic continental shelf. In the Atlantic this results in an increase of the bottom water salinity, while on a global average, the two effects nearly balance each other, with only a 0.01 psu increase of the bottom salinity in NSF.

The weak ventilation in the Southern Ocean induces a strong warming over the Antarctic continental shelf and of the AABW in NSF compared to CTR. Furthermore, the higher influence of relatively warm NADW in NSF contributes to a general warming of the ocean, with a maximum close to the bottom (+0.9°C at 5125 m on a global average).

Considering that sea ice has the same salinity as seawater does not directly impact on the sea ice in CLIO because it is assumed that the sea ice properties are not functions of salinity. Therefore any modification of the sea ice distribution must be caused indirectly by changes of the oceanic state. In the Northern Hemisphere the annual mean ice area and volume variations between the two experiments are modest: <1% and <2%, respectively (Table 2). In the Southern Ocean the annual mean ice area is 5% larger in NSF than in CTR (Table 2), the annual mean ice volume increasing by more than 20%. This higher ice volume is due to the weaker magnitude of the oceanic heat flux at the ice base during winter over a large portion of the Southern Ocean. The origin of this flux decrease is the absence of the destabilizing effect of the brine rejection in NSF, which induces weaker winter mixed layer depths in this experiment, except at some locations like the southeastern Pacific (see above). There the oceanic heat flux in winter is very high, and the ice concentration is much lower than in CTR or in the real world.

The conclusions drawn from the comparison between NSF and CTR concerning the changes in the Southern Ocean and their impact on the global circulation are in qualitative agreement with those of *Goosse et al.* 's [1997b] study, which specifically focused on AABW. Only some quantitative differences are noticed, probably because of the slightly different experimental design. On the other hand, *Stössel et al.* [1998] obtained in an experiment similar to NSF an intensification of the overturning cell close to Antarctica of 3 Sv compared to their reference experiment, in contradiction with the results presented here or by *Goosse et al.* [1997b]. They also observed a general increase in salinity close to Antarctica at great depths, while NSF (see Figure 10) and the experiment performed by *Goosse et al.* [1997b] display a strong freshening there. *Stössel et al.* [1998] argue that this difference could be caused by the fact that a surface salinity relaxation is applied in polar regions by *Goosse et al.* [1997b] but not in their experiment. Nevertheless, this argument seems not to be valid since results similar to *Goosse et al.* [1997b] are obtained in the present study, which does not use relaxation at high latitudes.

An alternative explanation of this discrepancy is the following. In the control experiment of *Stössel et al.* [1998], deep water renewal in the Southern Ocean occurs only in offshore regions through open ocean convection (this induces much too low an ice thickness in their experiments). Besides, shelf processes take an important part in deep water formation in CTR, in qualitative agreement with observations [*Foster and Carmack*, 1976; *Gordon*, 1991]. When the brine rejection due to ice formation is not accounted for, bottom water

Table 2. Summary of the Major Results of the Experiments

Experiment	Annual Mean Ice Area in Northern Hemisphere, km^2	Annual Mean Ice Area in Southern Hemisphere, km^2	NADW Exported at 30°S in the Atlantic, Sv	Maximum of the Overturning Cell close to Antarctica, Sv	AABW Inflow at 30°S in the Antlantic, Sv
CTR	11.5×10^6	12.5×10^6	18.1	33	6.4
NSF	11.3×10^6	13.1×10^6	19.4	19	6.2
LHT	13.0×10^6	15.4×10^6	15.2	30	4.6
FPT	11.7×10^6	15.2×10^6	18.9	32	4.4
STW	11.4×10^6	12.4×10^6	18.2	33	6.3

NADW, North Atlantic Deep Water; AABW, Antarctic Bottom Water.

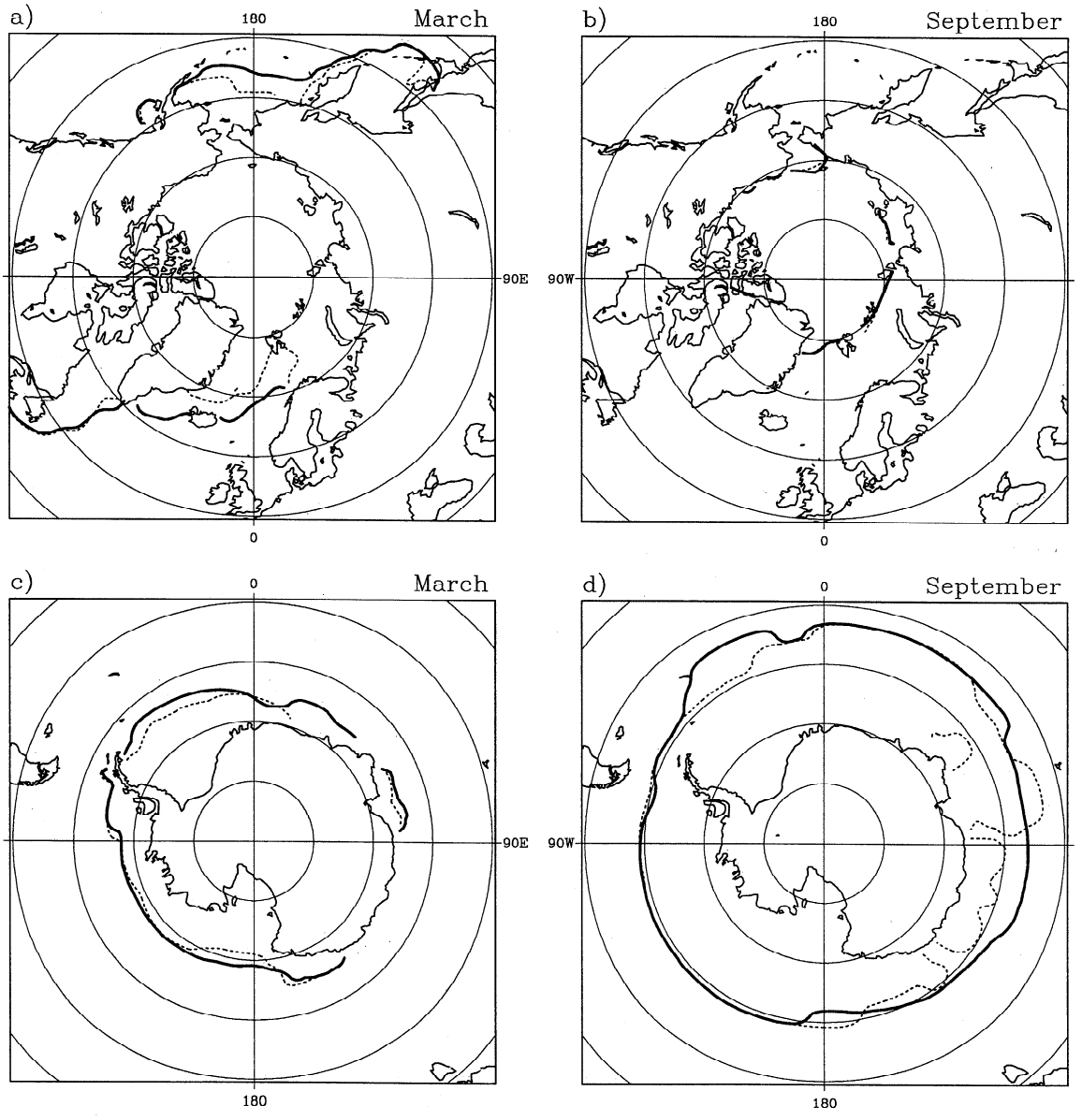

Figure 11. Location of the ice edge in LHT (solid lines) and CTR (dashed lines): (a) Northern Hemisphere in March, (b) Northern Hemisphere in September, (c) Southern Hemisphere in March, (d) Southern Hemisphere in September.

formation associated with shelf processes is suppressed, thus causing the weakening of the overturning close to Antarctica observed in NSF. On the other hand, in such a type of experiment, open ocean convection is still active and even intensifies at some locations. This could be the cause of the stronger overturning circulation in the Southern Ocean noticed by *Stössel et al.* [1998]. Furthermore, the characteristics of the bottom water formed by open ocean convection or near boundary convection are quite different [e.g., *Gordon*, 1991]. This gives a plausible explanation for the different evolution of deep salinity close to Antarctica in the sensitivity study of *Stössel et al.* [1998] compared to ours. The parameterization of downsloping flows included in our model could also play a role in the different behavior of the two models since it helps to export the dense water out of the continental shelf. Nevertheless, it could not be the only cause of the discrepancy since *Goosse et al.* [1997b] have the same kind of response as the one presented here even though no parameterization of downsloping flows is used and thus all the transport out of the continental shelf is achieved by the currents resolved by the model.

6. Influence of the Heat Exchange Between Ice and Ocean

6.1. Impact of a Decrease of the Heat Exchange Coefficient at the Ice-Ocean Interface

The purpose of this section is to study how the heat exchange between ice and ocean can affect the large-scale ocean circulation. To do so, an experiment (referred to as LHT) in which the coefficient of heat exchange between ice and ocean (c_h in (2)) has been reduced by a factor of 5 is performed with the goal of weakening significantly the ice-ocean heat transfer.

The most direct consequence of this modification is a larger ice coverage compared to CTR, mainly in winter (Figure 11). The annual mean ice area increases by 13% in the Northern Hemisphere and by 23% in the Southern Hemisphere (see Table 2). Although some changes occur nearly all along the ice edge, the ice advance is particularly pronounced in regions where a strong winter oceanic heat flux in CTR prevents ice from being maintained, as in the GIN Seas, the Bering Sea, or the Atlantic and Indian sectors of the Southern Ocean (see Figure 4). To illustrate this process, consider for instance the Norwegian and Greenland Seas. In this sector, there is a general southward ice transport. In CTR a large amount of the ice transported melts quickly thanks to the northward inflow of warm Atlantic waters between Iceland and Norway. As a consequence, ice can only be present close to Greenland (see Figure 2). In LHT, even if the same heat oceanic transport takes place, the heat is not transferred efficiently to the ice, which can be advected over a longer distance before melting. As a result, a significant part of the Norwegian and Greenland Seas becomes ice-covered in LHT.

The increase of the winter ice coverage in LHT tends to reduce the oceanic heat losses in these areas compared to CTR, the flux at the ice-ocean interface being generally weaker than at the ocean-atmosphere one. Because of these weaker heat losses, the ocean is warmer in LHT, with surface temperatures up to 1°C higher than in CTR in some areas, such as the Norwegian Sea or the continental shelf of Adélie Coast. At this stage it is useful to make a particular point concerning the model formulation. In our experiments the oceanic temperature below sea ice is not maintained equal to the freezing point. Nevertheless, the difference is generally small in CTR, as observed by *McPhee* [1992], since an oceanic temperature higher than the freezing point would induce a very strong oceanic heat flux and a large ice melting. In LHT this is not the case because of the decrease in c_h. Hence the temperature below the ice could be significantly greater than the freezing point. This leads to a kind of paradox associated with the low exchange coefficient: some regions are ice-covered in LHT and not in CTR, but the sea surface temperature there is higher in LHT.

This warm water is advected toward the interior of the ice pack in LHT. In some regions the warming is strong enough to compensate for the lower heat exchange coefficient, causing an enhanced sensible heat flux. For instance, the oceanic heat flux reaches 20 W m^{-2} in the Kara Sea during winter months in LHT, whereas it only amounts to a few W m^{-2} in CTR. This higher flux generates an overall decrease of ice thickness in both hemispheres in LHT. The more extensive ice coverage in LHT tends to increase the ice volume. Nevertheless, this contribution is overwhelmed by the impact of the general decrease of the ice thickness in LHT. As a consequence, the annual mean ice volume slightly decreases (-4% in the Northern Hemisphere; -1% in the Southern Hemisphere).

The reduction of the heat loss and the increase of the ocean surface temperature in the high latitudes of both hemispheres in LHT tend to reduce the surface density in those regions. As a result, convection weakens in the GIN Seas as well as in the Southern Ocean and is even completely stopped in the Labrador Sea. This is associated with a slower meridional circulation in LHT (see Figures 6c and 7c). In the North Atlantic the overturning in the GIN Seas is reduced by 1 Sv, and the maximum of the meridional stream function decreases from 26 Sv in CTR to 21 Sv in LHT. As a consequence, the export of NADW at 30°S out of the Atlantic is reduced by more than 3 Sv (18%). The maximum intensity of the overturning cell close to the Antarctic continent also decreases by 3 Sv in LHT. More significantly, the export of bottom water from the Southern Ocean toward the Atlantic, Indian, and Pacific basins at 30°S reaches 10 Sv in LHT compared to 17 Sv in CTR (i.e., a reduction of 41%). Qualitatively, the thermohaline circulation has not changed much in LHT compared to CTR (see Figures 6 and 7), with a geographical distribution of NADW and AABW being approximately the same in the two experiments, but the deep water ventilation has slowed down.

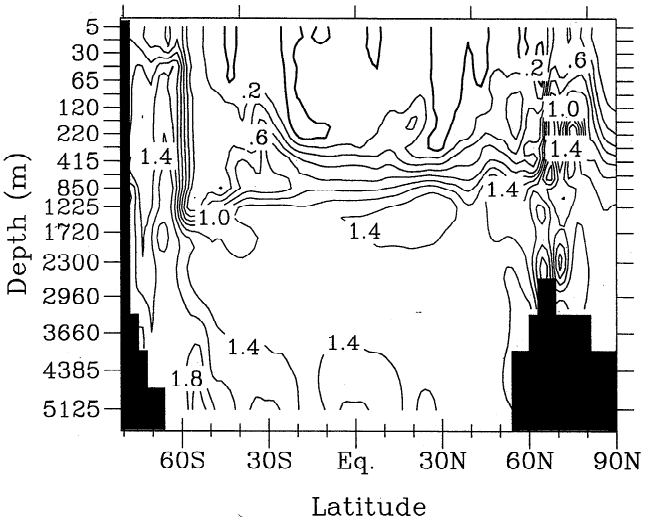

Figure 12. Difference of annual mean, zonally averaged temperature between LHT and CTR (LHT-CTR) in the global ocean. The contour interval is 0.2°C.

At the surface the temperature increase in LHT compared to CTR is restricted to polar regions (Figure 12), with almost no change between 50°N and 50°S. The surface signal in the high latitudes propagates at depth with the waters that are formed in these regions (mainly NADW and AABW). For instance, the temperature of the densest water in the Denmark Strait increases by 1.2°C in LHT. The slower ventilation of the deep ocean by these two water masses in LHT leads to an additional temperature increase of the deep ocean. The maximum warming reaches 2°C in the Southern Ocean close to the bottom. On a global average the temperature is 1.1°C higher in LHT.

LHT has shown that reducing the heat exchange coefficient between ice and ocean induces a significant increase of the Arctic and Antarctic ice extents and a decrease of the intensity of the global thermohaline circulation. Nevertheless, it is not straightforward to draw conclusions from this experiment on the influence of the heat flux at the ice-ocean interface in CLIO, in particular, because this flux decreases at some locations and increases at other ones in LHT. As a consequence, another experiment is presented in the next section in which there is a general decrease of the heat flux at the ice base.

6.2 Influence of a Modification of the Freezing Point Temperature

In FPT the freezing point temperature has been increased by 1°C, the heat exchange coefficient being the same as in CTR. As a result, the surface temperature below the ice is more or

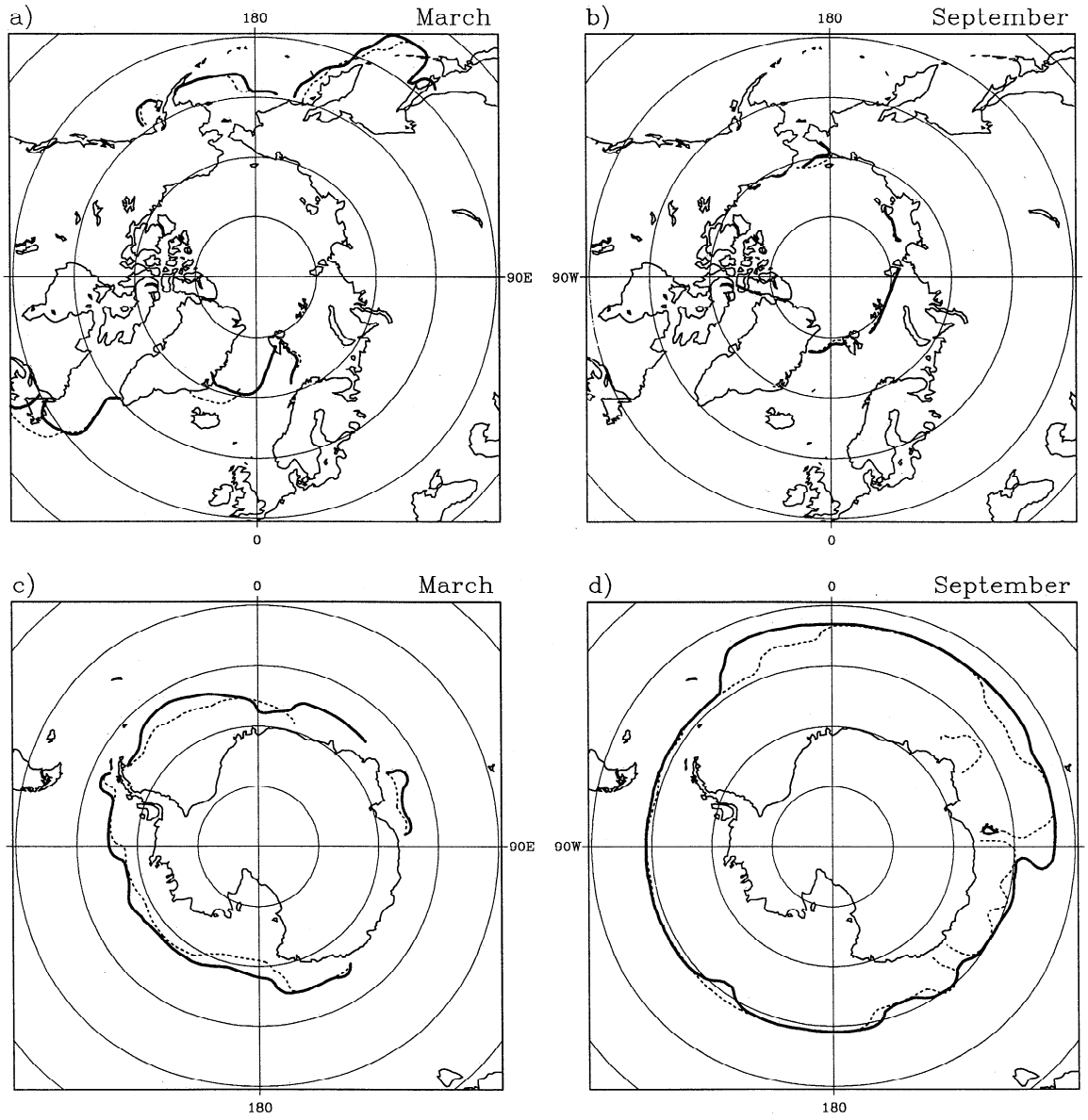

Figure 13. Location of the ice edge in FPT (solid lines) and CTR (dashed lines): (a) Northern Hemisphere in March, (b) Northern Hemisphere in September, (c) Southern Hemisphere in March, and (d) Southern Hemisphere in September.

less homogenous at a value of about -0.8°C, compared to -1.8°C in CTR. The changes of ice-ocean heat flux associated with this modification provide information that together with LHT, help to clarify the role of this flux in the large-scale circulation. Furthermore, it is possible in FPT to analyze the consequences of a systematic temperature change below the ice and to investigate how constraining the ocean surface temperature to remain close to the freezing point in polar regions affects the global ocean.

This change induces a decrease of the sensible heat flux at the ice base, with annual mean differences between 5 and 20 W m^{-2} in the Southern Ocean and generally lower than 10 W m^{-2} in the Northern Hemisphere. The basic mechanism responsible for this decrease is the following. The oceanic heat flux is mainly due to the transport of relatively warm water into the surface mixed layer, which is then cooled until its freezing point by contact with the sea ice. With a freezing point temperature higher by 1°C the amount of heat available at the ice base is reduced by a quantity equal to ρc_p x 1°C by m^3 of water. Consequently, the ice-ocean heat flux becomes weaker, the decrease depending on the magnitude of the flux of warm water into the surface mixed layer.

This lower heat flux and the ability of sea ice to form in water 1°C warmer than in CTR result in a larger ice extent in FPT, particularly in winter in the Atlantic and Indian sectors of the Southern Ocean (Figure 13). The differences are weaker in the Pacific Ocean at the same season, probably because the oceanic heat flux is already low there in CTR (see Figure 4). The Antarctic ice pack is also more extensive in summer at all longitudes. This results in an annual mean ice area higher by 22% in FPT than in CTR, the volume being larger by 31%. In the Northern Hemisphere the increase of 1°C of the freezing

point temperature is not sufficient to generate significant modifications of the position of the ice edge, with an increase of the annual mean ice area of only 2%. The increase of the ice volume is a little larger (8%).

The surface warming in polar regions is nearly 1°C on a zonal average (Figure 14a). Near Antarctica the warming signal is advected downward during bottom water formation, this warmer AABW being then advected northward. A secondary maximum of temperature change is noticed near the bottom in the North Atlantic. It is due to the larger influence of relatively warm NADW there in FPT compared to CTR (see Figure 6), a process that has already been described for NSF (section 5). Close to the NADW formation regions, the temperature changes are weak. The densest waters in Denmark Strait are only 0.1°C warmer in FPT than in CTR. It is hard to know if this corresponds to the inclusion of some water at the freezing point in NADW or if it is rather caused by a small modification of, for instance, convection patterns. Anyway, the major signal on deep ocean temperature comes from the Southern Ocean. On a global average the ocean temperature increases by 0.37°C in FPT. Again, this does not mean that 37% of the world ocean's water masses are produced at surface in ice-covered regions because some changes of circulation take place in FPT. However, this shows that increasing the freezing point temperature has a significant impact on the global ocean temperature.

The surface density change is weak in the Southern Ocean (Figure 14b) because the thermal expansion coefficient is very small close to the freezing point at low pressure. However, the temperature dependence of the density increases strongly with pressure, and the density significantly decreases close to the bottom in FPT compared to CTR, although the temperature difference is smaller than at the surface.

The modest changes of the surface density in the Southern Ocean generate a very weak slowing down of the Antarctic cell close to Antarctica, whose maximum intensity decreases by 1 Sv (see Figure 6d). However, the decrease of the density of AABW close to the bottom is responsible for a weaker propagation of this water mass in the Atlantic, the inflow decreasing by 2 Sv (see Table 2). The export of NADW at 30°S remains nearly unchanged (+0.8 Sv).

In the Southern Ocean, FPT and LHT are qualitatively similar. They both display an increase in ice extent, a decrease in the export of AABW, and a warming of the AABW. Besides, in the Northern Hemisphere the changes of ice extent and of deep water formation are very weak in FPT, while they are significant in LHT. In this hemisphere the perturbation of the heat fluxes and of the oceanic temperature are probably not strong enough in FPT to generate a significant modification of the oceanic circulation. To verify this hypothesis, an additional experiment has been performed in which the freezing point temperature has been enhanced by 2°C. In this experiment the ice extent increases strongly in both hemispheres. In particular, the ice covers a large part of the Norwegian and Labrador Seas. This results in a very significant decrease of NADW production and export, in qualitative agreement with the conclusions of LHT.

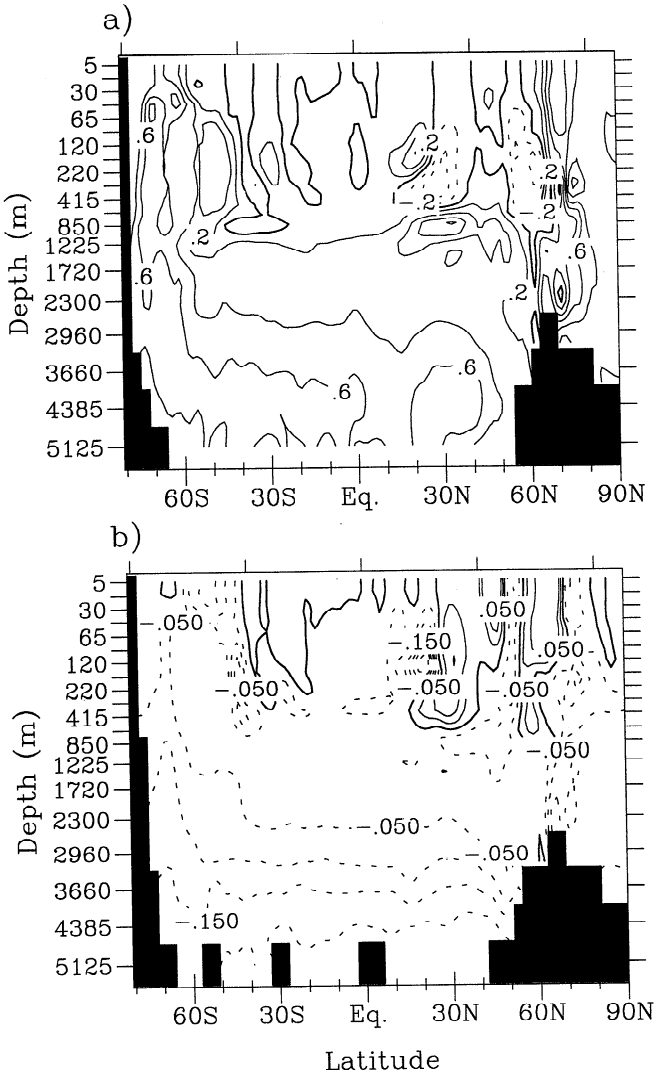

Figure 14. Difference of (a) annual mean, zonally averaged temperature in the global ocean and (b) density in the Atlantic Ocean between FPT and CTR (FPT-CTR). The contour intervals are 0.2°C in Figure 14a and 0.05 kg m^{-3} in Figure 14b.

7. Influence of the Momentum Exchange Between Ice and Ocean

In order to evaluate the impact of the ice interactions on the momentum exchanges between ice and ocean the climatological wind stress is applied directly at the top of the ocean in experiment STW. It must be noticed that this stress at the ocean surface in STW is not the one that would occur if no ice were present. Indeed, in the derivation of the climatological stress, *Trenberth et al.* [1989] use a higher drag coefficient in polar regions to take into account the higher roughness of the ice. STW actually represents an idealized situation in which the stress at the top of the ice-ocean system is transferred to the ocean without modification due to internal ice stress or other effects inside the ice pack. To compute the stress at the ice base, (1) is still used but with the oceanic velocities obtained in CTR. This method has been chosen because using the ocean velocities from experiment STW would induce a stronger ice transport. This would affect the heat and salt/freshwater fluxes at the ice-ocean interface and make the analysis of the influence of momentum exchanges alone much more difficult. As a result, the ice dynamics do not feel any impact of the changes of ocean surface stress in STW, and the ice velocities are nearly identical in CTR and STW.

In most of the Southern Ocean the internal ice stress is generally weak, the dynamic equilibrium of the ice being

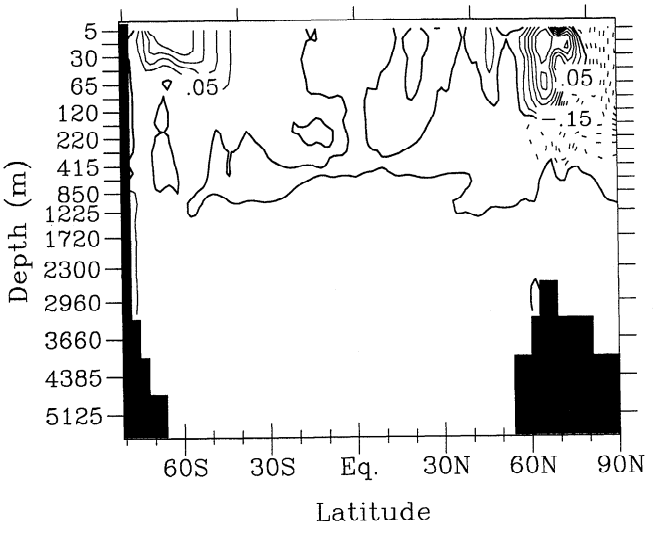

Figure 15. Difference of annual mean, zonally averaged salinity in the global ocean between stress at ocean surface equal to wind stress experiment (STW) and CTR (STW-CTR). The contour interval is 0.05 psu.

mainly between air-ice and ice-ocean stresses. The only exceptions are the southwestern Weddell Sea and the Amundsen-Bellingshausen Seas. There, because of ice convergence, the ice-ocean stress is significantly lower in CTR than the air-ice stress, with a maximum decrease of 90% in some areas during winter. The ice-ocean stress has also a much smaller magnitude than the air-ice stress in the central Arctic because of the strong ice interactions: the reduction exceeds 50% all year long in CTR, with a maximum in winter. In the GIN Seas or the Labrador Sea the decrease is smaller as the ice is less compact.

Since the air-ice stress can be significantly larger than the air-ocean stress in some regions in CTR, applying directly the wind stress at the ocean surface in STW modifies locally the oceanic circulation. The intensity of the cyclonic gyre in the Bellingshausen and Amundsen Seas more than doubles (~50 Sv in STW compared to 20 Sv in CTR), and the strength of the Weddell Gyre increases by 5 Sv in STW. The anticyclonic circulation in the central Arctic also accelerates (by a little more than 1 Sv). This is associated with a decrease of salinity in the central Arctic pycnocline, while the surface salinity off the Canadian Archipelago, as in Baffin Bay, increases up to 0.5 psu on an annual average. The changes are even more dramatic in the Bellingshausen Sea, where the sea surface temperature and salinity increase in STW reach 1.2°C and 0.8 psu, respectively. Nevertheless, these modifications of upper ocean properties occur in regions that appear not to be critical for the global ocean circulation in the model, and they remain mainly confined to the first hundred meters of the polar oceans (Figure 15). The meridional oceanic circulation is virtually unchanged, with the amount of NADW exported into the Southern Ocean and the intensities of the counterclockwise cells close to Antarctica and near the ocean bottom all changing by <0.5 Sv (see Table 2). The meridional overturning stream function is so close to the one of CTR that they have not been displayed in Figures 6 and 7.

In our experiment the global effect of the modification by ice of the oceanic surface stress compared to the wind stress is very weak. However, *Toggweiller and Samuels* [1995b] have argued that the wind-driven upwelling in the latitude band containing the Drake Passage might remove deep water and has an influence on the NADW production and export. For present-day conditions it appears that the ice cover has nearly no impact on the ocean stress in this region, but the situation could have been quite different in the past. For instance, during the Last Glacial Maximum, ~21,000 years ago, the ice pack extented much more north than today in the Southern Ocean and occupied a significant part of the latitude band of the Drake Passage [*Climate: Long-Range Investigation Mapping and Prediction (CLIMAP),* 1981]. As a consequence, sea ice could have modified the surface stress there and might have had an influence on the thermohaline circulation. This hypothesis is quite speculative, but it probably deserves some attention.

8. Conclusions

In this study the importance for the global ocean circulation of the exchanges of heat, salt/freshwater, and momentum between sea ice and ocean has been investigated with a coarse-resolution ice-ocean model. To achieve this goal, numerical experiments in which the influence of each of these interactions is isolated as much as possible have been carried out and compared to a control experiment (CTR) taking into account all those processes. The conclusions drawn from these simulations are quite different between the two hemispheres.

In the Southern Ocean the ice-ocean exchanges of heat and salt/freshwater appear to be crucial for deep water formation. First, the brine rejected during ice formation on the Antarctic continental shelf allows the shelf water to be dense enough to sink to the bottom, contributing to the renewal of AABW. If this process is neglected (NSF), the salinity on the Antarctic continental shelf decreases by >1 psu. Therefore this mode of AABW formation is totally suppressed, inducing a weakening of the AABW export and a warming of the deep ocean (+0.9°C on a global average close to the bottom). On the other hand, the ice transport convergence in some areas, as in the southeastern Pacific, leads to net ice melting that stabilizes the water column and forbids open ocean convection. As a consequence, open ocean convection is enhanced in these zones in NSF. A mechanism linking convection on the shelf and in the open ocean has been suggested by *Gordon* [1982] and *Martinson* [1991] to explain some interannual variabilities in the production of bottom water. During years of intense ice divergence on the shelf the high salinity there allows export of dense water along the shelf slope, but a large amount of ice is transported toward the open ocean, where it tends to stabilize the water column. Besides, during years of low ice divergence on the shelf the opposite would occur, with a reduction of the bottom water production near the shelf and an intensification of the convection in the open ocean. Our results are compatible with this kind of mechanism even if a detailed observational confirmation needs to be performed.

Second, the cooling of the water by contact with the ice until its freezing point contributes significantly to increasing the density of surface waters. If the heat exchange between ice and ocean is reduced or if the freezing point temperature is increased in a sensitivity experiment, the surface waters become warmer and thus less dense. As a consequence, deep water renewal becomes slower in the Southern Ocean,

resulting in a slower export of AABW in LHT and FPT than in CTR. These modifications induce a noticeable warming of the deep ocean (>1°C close to the bottom in LHT and FPT). Those sensitivity experiments also display a pronounced increase of the ice extent in the Southern Ocean.

Besides, the NADW formation in our model seems to be due to the intense oceanic cooling at the ocean-atmosphere interface in the Labrador Sea and GIN Seas. Even if convection takes place close to the ice edge, the ice-ocean interactions play at best a secondary role. A significant modification in the NADW production rate is only found in the experiment in which a decrease of the heat exchange coefficient at the ice-ocean interface (LHT) leads to a significant increase in ice extent. In this experiment the zone of NADW formation becomes partly ice-covered. This isolates the ocean from the atmosphere, reducing the oceanic heat loss and the rate of NADW production there.

In the control experiment a significant amount of freshwater is transported by sea ice from the Arctic to the GIN Seas through Fram Strait. When neglecting the salt/freshwater exchanges between ice and ocean (NSF), this ice motion is not associated with a freshwater transport. Nevertheless, by a compensating mechanism the southward freshwater transport by the ocean currents at Fram Strait increases by roughly the amount due to the ice transport in CTR. As a consequence, surface salinity and convection in the GIN Seas is not sensibly altered at equilibrium. This does not mean that the amount of freshwater exchange between the Arctic and the GIN Seas is not important for deep water renewal. Indeed, several studies performed with this model [e.g., *Goosse et al.*, 1997a] have shown that variations of the total freshwater inflow from the Arctic affects significantly the convection in the GIN Seas. It simply says that in our experiments it seems not to be very important for NADW formation that this freshwater is carried out by the ocean or by the ice.

The wind patterns in the high latitudes are very important for the global oceanic circulation. For instance, they determine to a large extent the zones of ice convergence or divergence and thus the net ice melting or freezing, which is a crucial element for deep water formation. By contrast, the modification of momentum exchange between atmosphere and ocean by the presence of an ice cover seems to have no impact at the global scale in the model. In STW the wind stress is applied directly at the ocean surface. This perturbation has pronounced local effects but nearly no impact on deep water production and export or even on the annual mean ice area. Nevertheless, this conclusion is valid only if CTR is used as a control experiment. It is possible that under different conditions, an experiment equivalent to STW would generate significant changes in some polar regions important for the world ocean's circulation and thus would have a global influence.

Caution must be exercised when interpretating our experiments. First of all, the results are only valid for the equilibrium state and do not take into account interannual variability. If, for instance, the ice transport at Fram Strait increases during a particular year, this would not be instantaneously balanced by a weaker freshwater transport in the ocean. As a consequence, the enhanced freshwater transport could induce a surface salinity decrease in the GIN Seas and forbid deep water production there for a certain period [e.g., *Häkkinen*, 1993]. Furthermore, because of the coarse grid of the model, only the large-scale response of the ice-ocean system can be studied, and even this large-scale response suffers from the model inaccuracies. If a process depends critically on features occurring at small scales, it cannot be investigated in the present framework. For instance, some authors have suggested that brine released during ice formation can precondition the water column for deep water formation in the North Atlantic [e.g., *Visbeck et al.*, 1995]. It appears that this process is not of prime importance in our simulations. However, our experiments cannot rule out or prove that this preconditioning plays a role at a smaller horizontal scale than the one resolved by our coarse-grid model. The use of monthly mean forcing can also pose problems, particularly for the kind of preconditioning suggested by *Visbeck et al.* [1995], since it seems to depend strongly on the high frequency variability of the forcing.

Another important point is the nonlinear response of the ice-ocean system in our experiments. One example is the increase in bottom salinity when neglecting the salt/freshwater exchanges between ice and ocean (NSF). In this experiment the salt transfer from the Antarctic continental shelf to the deep ocean is suppressed, but this is more than compensated for by a higher inflow of relatively salty NADW to great depths. A second example is the decrease of the ice volume in LHT. This is caused by an increase of the oceanic temperature at some locations, which overwhelms the effect of the lower heat exchange coefficient, leading to an increase of the sensible heat flux at the ice base. Those examples show that it is necessary to be careful when anticipating the response of the ocean-ice system to a perturbation and that the analysis of such a response must take into account the possible feedbacks inside the system.

In the sensitivity experiments conducted in this study the atmospheric properties are supposed to be fixed. This implicitly assumes that the major changes between the experiments concern the ocean and sea ice, which seems natural considering the processes investigated. Nevertheless, this hypothesis tends to underestimate the response of the modeled sea ice to perturbations since a decrease of the ice extent is generally associated with an increase of the temperature (mainly because of the temperature-albedo feedback) which yields to a further decrease of the ice extent. On the other hand, some stabilizing feedbacks, such as the one described by *Rahmstorf and Willebrand* [1995] could also take place in the atmosphere–ocean–sea ice system. A natural prolongation of this study would thus be to investigate how the processes presented here would be amplified or damped when considering an interactive atmosphere. Despite all the above-mentioned limitations, our results suggest that the large-scale ice-ocean interactions take an important part in controlling the world ocean's circulation, so their treatment in global climate models should be considered with care.

Acknowledgments. We want to thank J.-M. Campin, H. Cattle, D. Martinson, A. Stössel, and B. Tartinville for very interesting discussions about this work. The comments of three anonymous reviewers were very much appreciated. H. Goosse and T. Fichefet are sponsored by the National Fund for Scientific Research, Belgium. This work was done within the scope of the Global Change and Sustainable Development Programme (Belgian State, Prime Minister's Services, Federal Office for Scientific, Technical, and Cultural Affairs, contract CG/DD/09A), the Convention d'Actions de Recherche Concertées ARC 97/02-208 (Communauté Française de Belgique), and the Environment and Climate Programme (European Commission, contract ENV4-CT95-0102). All of these funding agencies are gratefully acknowledged. We also want to thank the different data centers that provided us with the forcing data (see references in the text), particularly the Global Runoff Data Center, Koblenz (Germany).

References

Aagaard, K., and E. Carmack, The role of sea ice and other fresh water in the Arctic circulation, *J. Geophys. Res.*, *94*, 14,485-14,498, 1989.

Baumgartner, A., and E. Reichel, *The World Water Balance*, 179 pp., Elsevier, New York, 1975.

Berliand, M.E., and T.G. Strokina, *Global Distribution of the Total Amount of Clouds* (in Russian), 71 pp., Hydrometeorol. Pub. House, Leningrad, Russia, 1980.

Bourke, R.H., and A.S McLaren, Contour mapping of Arctic basin ice draft and roughness parameters, *J. Geophys. Res.*, *97*, 17,715-17,728, 1992.

Budd, W.F., Antarctica and global change, *Clim. Change*, *18*, 272-299, 1991.

Campin, J.-M., and H. Goosse, A parameterization of density-driven downsloping flow for a coarse-resolution model in *z*-coordinate, *Tellus , Ser. A*, *51*, 412-430, 1999.

Cattle, H., Diverting soviet rivers: Some possible repercussions for the Arctic Ocean, *Polar Record*, *22*, 485-498,1985.

Climate: Long-Range Investigation, Mapping, and Prediction (CLIMAP) Project Members, Seasonal reconstruction of the Earth's surface at the Last Glacial Maximum, *Geol. Soc. Am. Map Chart Series*, *36*, 1981.

Comiso, J.C., and A.L. Gordon, Recurring polynyas over the Cosmonaut Sea and the Maud Rise, *J. Geophys. Res.*, *92*, 2819-2833, 1987.

Crutcher, H.L., and J.M. Meserve, Selected level heights, temperatures and dew points for the Northern Hemisphere, *NAVAIR Rep. 50-1C-52*, revised, U.S. Nav. Weather Serv. Command, Washington, D.C., 1970.

Deleersnijder, E., and J.-M. Campin, On the computation of the barotropic mode of a free-surface World Ocean model, *Ann. Geophys. 13*, 675-688, 1995.

England, M.H., and A.C. Hirst, Chlorofluorocarbon uptake in a World Ocean model, 2, Sensitivity to surface thermohaline forcing and subsurface mixing parameterisations, *J. Geophys. Res.*, *102*, 15,709-15,731, 1997.

Fichefet, T., and H. Goosse, A numerical investigation of the spring Ross Sea polynya, *Geophys. Res. Lett.*, *26*, 1015-1018, 1999.

Fichefet, T., and M. A. Morales Maqueda, Sensitivity of a global sea ice model to the treatment of ice thermodynamics and dynamics, *J. Geophys. Res.*, *102*, 12,609-12,646, 1997.

Foster, T.D., and E.C. Carmack, Frontal zone mixing and Antarctic Bottom Water formation in the southern Weddell Sea, *Deep Sea Res., Part I, 23*, 301-317, 1976.

Gloersen, P., W.J. Campbell, D.J. Cavalieri, J.C. Comiso, C.L. Parkinson, and H.J. Zwally, Arctic and Antarctic sea ice, 1978-1987: Satellite passive-microwave observations and analysis, *NASA Spec. Publ., 511*, 290 pp., 1992.

Goosse, H., Modelling the large-scale behaviour of the coupled ocean–sea-ice system, Ph.D. thesis, 231 pp., Fac. des Sci. Appl., Univ. Cath. de Louvain, Louvain-la -Neuve, Belgium, 1997.

Goosse, H., J.M. Campin, T. Fichefet, and E. Deleersnijder, Sensitivity of a global ice–ocean model to the Bering Strait throughflow, *Clim. Dyn.*, *13*, 349-358, 1997a.

Goosse, H., J.M. Campin, T. Fichefet, and E. Deleersnijder, The impact of sea-ice formation on the properties of Antarctic Bottom Water, *Ann. Glaciol.*, *25*, 276-281, 1997b.

Goosse, H., E. Deleersnijder, T. Fichefet, and M.H. England, Sensitivity of a global coupled ocean-sea ice model to the parameterization of vertical mixing, *J. Geophys. Res.*, *104*, 13,681-13,695, 1999.

Gordon A.L., Weddell Deep Water variability, *J. Mar. Res.*, *40* , suppl., 199-217, 1982.

Gordon, A.L., Two stable modes of Southern Ocean winter stratification, in *Deep Convection and Deep Water Formation in the Oceans*, *Elsevier Oceanogr. Ser. 57*, edited by P.C. Chu and J.C. Gascard, pp. 17-35, Elsevier, New York, 1991.

Gordon, A.L., and B.A. Huber, Southern Ocean winter mixed layer, *J. Geophys. Res.*, *95*, 11,655-11,672, 1990.

Grabs, W., T. De Couet, and J. Pauler, Freshwater fluxes from continents into the world oceans based on data of the global runoff data base, *Global Runoff Data Cent. Rep. 10*, 228 pp., Fed. Inst. of Hydrol., Koblenz, Germany, 1996.

Häkkinen, S., An Arctic source for the great salinity anomaly: A simulation of the Arctic ice-ocean system for 1955-1975, *J. Geophys. Res.*, *98*, 16,397-16,410, 1993.

Hellerman, S., and M. Rosenstein, Normal monthly wind stress over the World Ocean with error estimates, *J. Phys. Oceanogr.*, *13*, 1093-1104, 1983.

Hibler, W.D., A dynamic thermodynamic sea ice model, *J. Phys. Oceanogr.*, *9*, 815-846, 1979.

Hibler, W.D., and K. Bryan, A diagnostic ice-ocean model, *J. Phys. Oceanogr.*, *17*, 987-1015, 1987.

Holland, D.M., L.A. Mysak, and J.M. Oberhuber, Simulation of the mixed-layer circulation in the Arctic Ocean, *J. Geophys. Res.*, *101*, 1111-1128, 1996.

Holland, M.M., J.A. Curry and J.L. Schramm, Modeling the thermodynamics of a sea ice thickness distribution. 2. Sea ice/ocean interactions, *J. Geophys. Res.*, 102, 23,093-23,107, 1997.

Houghton, J.T., L.G. Meira Filho, B.A. Callander, N. Harris, A. Kattenberg, and K. Maskell (Eds.), *Climate Change 1995: The Science of Climate Change*, Intergovernmental Panel on Climate Change, 572 pp., Cambridge Univ. Press, New York, 1996.

Jaeger, L., Monatskarten des niederschlags für die ganze Erde (in German), *Ber. Dtsch. Wetterdienstes*, *139*, 38 pp., 1976.

Killworth, P.D., Deep convection in the World Ocean, *Rev. Geophys.*, *21*, 1-26, 1983.

Kim, S.J., and A. Stössel, On the representation of Southern Ocean water masses in an ocean climate model, *J. Geophys. Res.*, *103*, 24,891-24,906, 1998.

Legates, D.R., and C.J. Willmott, Mean seasonal and spatial variability in gauge-corrected, global precipitation, *Int. J. Clim.*, *10*, 111-127, 1990.

Legutke, S., E. Maier-Reimer, A. Stössel, and A. Hellbach, Ocean–sea-ice coupling in a global ocean general circulation model, *Ann. Glaciol.*, *25*, 116-120, 1997.

Levitus, S., Climatological atlas of the World Ocean, *Prof. Pap. 13*, 173 pp., Natl. Oceanic and Atmos. Admin., U.S. Dep. of Comm., Washington, D.C., 1982.

Lytle, V.I., and S.F. Ackley, Heat flux through sea ice in the western Weddell Sea: Convective and conductive transfer processes, *J. Geophys. Res.*, *101*, 8853-8868, 1996.

Macdonald, A.M., and C. Wunsch, An estimate of global ocean circulation and heat fluxes, *Nature*, *382*, 436-439, 1996.

Martinson, D.G., Evolution of the Southern Ocean winter mixed layer and sea ice: Open ocean deepwater formation and ventilation, *J. Geophys. Res.*, *95*, 11,641-11,654, 1990.

Martinson, D.G., Open ocean convection in the Southern Ocean, in *Deep Convection and Deep Water Formation in the Oceans*, *Elsevier Oceanogr. Ser. 57*, edited by P.C. Chu and J.C. Gascard, pp. 37-52, Elsevier, New York, 1991.

Mauritzen, C., Production of dense overflow waters feeding the North Atlantic across the Greenland-Scotland Ridge, 1, Evidence for a revised circulation scheme, *Deep Sea Res., Part I, 43*, 769-806, 1996.

McPhee, M.G., Turbulent heat flux in the upper ocean under sea ice, *J. Geophys. Res.*, *97*, 5365-5379, 1992.

McPhee, M.G., and N. Untersteiner, Using sea ice to measure heat flux in the ocean, *J. Geophys. Res.*, *87*, 2071-2074, 1982.

Mellor, G.L., and T. Yamada, Development of a turbulence closure model for geophysical fluid problems, *Rev. Geophys.*, *20*, 851-875, 1982.

Morawitz, W.M.L., P.J. Sutton, P.F. Worcester, and B.D. Cornuelle, Three-dimensional observations of a deep convective chimney in the Greenland Sea during winter 1988/1989, *J. Phys. Oceanogr.*, *26*, 2316-2343, 1996.

Rahmstorf, S., and J. Willebrand, The role of temperature feedback in stabilizing the thermohaline circulation, *J. Phys. Oceanogr.*, *25*, 787-805, 1995.

Schmitz, W.J., On the interbasin-scale thermohaline circulation, *Rev. Geophys.*, *33*, 151-173, 1995.

Steele, M., D. Thomas, D. Rothrock, and S. Martin, A simple model study of the Arctic Ocean freshwater balance 1979-1985, *J. Geophys. Res.*, *101*, 20,833-20,848, 1996.

Steele, M., J. Zhang, D. Rothrock, and H. Stern, The force balance of sea ice in a numerical model of the Arctic Ocean, *J. Geophys. Res.*, *102*, 21,061-21,079, 1997.

Stössel, A., P. Lemke, and W.B. Owens, Coupled sea ice–mixed layer simulations for the Southern Ocean, *J. Geophys. Res.*, *95*, 9539-9555, 1990.

Stössel, A., S.J. Kim, and S.S. Drijfout, The impact of Southern Ocean sea ice in a global ocean model, *J. Phys. Oceanogr.*, *28*, 1999-2018, 1998.

Taljaard, J.J,. H. van Loon, H.L. Crutcher, and R.L. Jenne, Climate of the upper air, I, Southern Hemisphere, vol. 1, Temperatures, dew points, and heights at selected pressure levels, *NAVAIR 50-1C-55*, 135 pp., U.S. Nav. Weather Serv., Washington, D.C., 1969.

Thomas, D., S. Martin, D. Rothrock, and M. Steele, Assimilating satellite concentration data into an Arctic sea ice mass balance model, 1979-1985, *J. Geophys. Res., 101*, 20,849-20,868, 1996.

Toggweiler, J.R., and B. Samuels, Effect of sea ice on the salinity of Antarctic Bottom Waters, *J. Phys. Oceanogr., 25*, 1980-1997, 1995a.

Toggweiler, J.R., and B. Samuels, Effect of Drake Passage on the global thermohaline circulation, *Deep-Sea Res., Part I, 42*, 477-500, 1995b.

Trenberth, K.E., J.G. Olson, and W.G. Large, A global ocean wind stress climatology based on ECMWF analyses, *NCAR/TN-338 +STR*, 93 pp., Nat. Cent. for Atmos. Res., Boulder, Colo., 1989.

Visbeck, M., J. Fischer, and F. Schott, Preconditioning the Greenland Sea for deep convection: Ice formation and ice drift, *J. Geophys. Res., 100*, 18,489-18,502, 1995.

Xie, P., and P. A. Arkin, Analyses of global monthly precipitation using gauge observations, satellite estimates and numerical model predictions, *J. Clim., 9*, 840-858, 1996.

T. Fichefet and H. Goosse, Institut d'Astronomie et de Géophysique G. Lemaître (ASTR), Université Catholique de Louvain, 2 Chemin du cyclotron, B-1348, Louvain-la-Neuve, Belgium. (hgs@astr.ucl.ac.be)

(Received October 26, 1998; Revised July 5, 1999;
accepted July 13, 1999)